A bacterial endosymbiont enables fungal immune evasion during fatal mucormycete infection

Herbert Itabangi[1], Poppy C. S. Sephton-Clark[1], Xin Zhou[1], Ignacio Insua[2], Mark Probert[1], Joao Correia[1], Patrick Moynihan[1], Teklegiorgis Gebremariam[3], Yiyou Gu[3], Lin Lin[3], Ashraf S. Ibrahim[3], Gordon D. Brown[4], Jason S. King[5], Francisco Fernandez Trillo[2], Elizabeth R. Ballou[1*], Kerstin Voelz[1*]

[1]*Institute of Microbiology and Infection, School of Biosciences, University of Birmingham, Edgbaston, Birmingham, B15 2TT, UK*

[2]*School of Chemistry, University of Birmingham, Edgbaston, Birmingham, B15 2TT, UK.*

[3]*Division of Infectious Diseases, David Geffen School of Medicine, UCLA, Los Angeles Biomedical Research Institute, Harbor-UCLA Medical Center, Torrance, California, U.S.A.*

[4]*Medical Research Council Centre for Medical Mycology at the University of Aberdeen, Aberdeen Fungal Group, Foresterhill, Aberdeen, AB25 2ZD, UK*

[5]*Department of Biomedical Science, University of Sheffield, Western Bank, Sheffield, S10 2TN, UK.*

***** To whom correspondence should be addressed
ERB: e.r.ballou@bham.ac.uk
KV: dr.kerstin.voelz@gmail.com

Funding support:
This work was supported by a Wellcome Trust Seed award to KV (108387/Z/15/Z). HI is supported by the Wellcome Trust Strategic Award in Medical Mycology and Fungal Immunology (097377). PCSC is supported by a BBSRC MIBTP PhD Studentship (BB/M01116X/1). XZ is supported by a Studentship from the Darwin Trust of Edinburgh. MP was supported by a British Mycological Undergraduate Student Bursary. PM is supported by the UK Biotechnology and Biological Research Council (BB/S010122/1). ASI is supported by Public Health Service grants from the National Institutes of Allergy and Infectious Diseases R01 AI063503. Funding for GDB was provided by the Wellcome Trust (102705, 097377) and the MRC Centre for Medical Mycology and the University of Aberdeen (MR/N006364/1) JSK is supported by Royal Society University Research Fellowship UF140624. FFT and II were supported by the University of Birmingham (John Evans Fellowship to FFT). ERB was supported by the UK Biotechnology and Biological Research Council (BB/M014525/1) and a Sir Henry Dale Fellowship jointly funded by the Wellcome Trust and the Royal Society (211241/Z/18/Z).

Author Contributions:
HI designed the experiments, performed the work, performed the analysis, and wrote the manuscript.
PCSC designed the experiments, collected the data, performed the analysis, contributed to the interpretation, and contributed to the manuscript.

XZ contributed to the acquisition and analysis of data and contributed to the manuscript.
II contributed to the acquisition and analysis of data and contributed to the manuscript.
MP contributed to the acquisition and analysis of data and contributed to the manuscript.
JC contributed to the acquisition and analysis of data and contributed to the manuscript.
PM contributed to the experimental design and acquisition and analysis of data and contributed to the manuscript.
TG contributed to the acquisition and analysis of data and contributed to the manuscript.
YG contributed to the acquisition and analysis of data and contributed to the manuscript.
LL contributed to the acquisition and analysis of data and contributed to the manuscript.
BP contributed to the acquisition and analysis of data and contributed to the manuscript.
ASI contributed to the experimental design and interpretation and contributed to the manuscript.
GB contributed to the experimental design and interpretation and contributed to the manuscript.
JSK contributed to the experimental design and interpretation and contributed to the manuscript.
FFT contributed to the experimental design and interpretation and contributed to the manuscript.
ERB contributed to the experimental design, analysis and interpretation of data and wrote the manuscript.
KV conceived and designed the experiments, contributed to the analysis and interpretation of data, and wrote the manuscript.

Abstract

Environmentally ubiquitous fungal spores of the Mucorales order cause acute invasive infections through germination and evasion of the mammalian host immune system. Early phagocyte control of spore germination plays a key role in controlling infection, yet swelling Mucorales spores evade phagocytosis through an unknown mechanism. Here we investigate fungal immune evasion in a clinical isolate of *Rhizopus microsporus* and reveal the role of a bacterial endosymbiont, *Ralsonia pickettii,* in fungal pathogenesis. Analysis of phagocytosis rates in wild type and cured fungal isolates demonstrates a role for the endosymbiont in immune cell evasion through disruption of the cytoskeleton and phagosome maturation. Further analysis of bacterial secreted products revealed the presence of a previously uncharacterized secondary metabolite whose production is induced by the presence of the fungus. Analysis of the bacterial genome and condition-dependent RNAseq implicate a cryptic type I polyketide synthase. Subsequent analysis of wild type and cured spores in a zebrafish larvae model of infection demonstrate a role for the endosymbiont in suppressing macrophage and neutrophil recruitment to the site of infection. Finally, we demonstrate that this has implications for fungal clearance in an immunocompetent murine model of infection. Together, these findings identify for the first time a role for a bacterial endosymbiont in the pathogenesis of *Rhizopus microsporus* during animal infection.

Introduction

The innate immune response is a key component of the host defense against fungal infection, and fungi have developed diverse mechanisms to evade phagocyte-mediated clearance[1]. Pathogenic fungi mask key cell wall ligands to evade uptake[2-6]. Upon engulfment, they deploy various strategies to proliferate within and escape the phagolysosome, or switch morphology to resist phagocyte killing[7-15]. This is particularly true with *Aspergillus fumigatus* spores, which mask key cell wall ligands when in a resting state[16,17]. Mucoralean fungi that cause invasive mucormycoses lack many of these strategies, yet remain an important class of fungal pathogens with high mortality in susceptible patient populations[18-20]. Pathogenic Mucorales span multiple genera, with members of the *Rhizopus* genus most prevalent, causing almost half of all documented cases[21-25]. Mucorales virulence has been shown to be affected by spore size and immunogenicity, germination rate, hyphal biomass, and hyphal resistance to killing[26-30]. The species *Rhizopus microsporus* is among the most frequent causes of mucormycosis[31,32], but fails to mask cell wall ligands in swollen spores, has a slow germination rate, and produces relatively low biomass[26,33]. This raises questions about how *R. microsporus* evades the innate immune response to cause disease.

During Mucorales infection, swollen spores form germlings, which adhere to and penetrate endothelial cells, rapidly invade blood vessels, and disseminate, causing necrosis[34-37]. Treatment requires debridement or amputation in combination with antifungal therapy and mortality rates approach 100% in disseminated cases[21,38]. There are also emerging reports of indolent/chronic mucormycoses in both immunocompromised and immunocompetent patients[39,40]. Given this pressing problem, the focus of Mucorales pathogenesis studies has been on disseminated disease, particularly hyphal resistance to host immunity, a hallmark of pathogenicity. However, we recently showed that the early stages of infection control are critical for predicting disease outcome[41]. Consistent with this, the majority of mucormycosis patients have predisposing factors that impact phagocyte recruitment, including iron overload, diabetes mellitus, neutropenia, organ transplantation, trauma, and corticosteroid

therapy[19,22,34,42-50]. Outbreaks of *R. microsporus* in hospitals have been linked to the use of contaminated supplies during treatment of immunocompromised patients[51-55]. Among the 19% of cases that occur in patients with otherwise competent immune systems, chronic local injury appears to be a predisposing factor[21]. Together, these findings emphasize the importance of a robust innate immune response early during infection, and urge further study of the initial stages of infection.

Mucormycete plant pathogens, including the Mucorales, are colonized by bacterial endosymbionts of the genera *Burkholderia* and *Ralstonia*, closely related to the *Pseudomonas* genus[35,56]. These endosymbionts influence fungal behavior such as growth and sporulation, and also mediate plant pathogenesis[57,58]. The endotoxin Rhizoxin inhibits plant defenses and is secreted by *Burkholderia rhizoxina* during mutualism with its fungal host *Rhizopus microsporus*[59,60]. However, a role for endosymbionts in mammalian disease has not been established. Previous work demonstrated that endosymbionts are wide spread in patient samples, but diabetic mouse models of infection found no role for the endosymbiont in disease progression[35].

Recently, we showed that recruitment of phagocytes to the site of infection enables the formation of a granuloma that can contain and control the germination of resting *Mucor circinelloides* spores[41]. In contrast, a range of Mucorales resting spores fail to elicit pro-inflammatory cytokine responses and do not induce the strong phagocyte chemotaxis required for granuloma formation[33,61-63]. *R. microsporus* spores are also phagocytosed at lower rates than other well studied fungal spores[40,62,64,65]. This raises the question of what role early immune recruitment has in the control of *Rhizopus* infection.

Upon infection, *R. microsporus* spores become metabolically active and begin to swell[61,66]. Based on analogy to *Aspergillus* species, frequently used as a model for Mucorales, swelling would be expected to reveal Pathogen Associated Molecular Patterns (PAMPs) and induce increasing rates of phagocytosis[2,67]. However, swollen spores in the *Rhizopus* genus are often no more readily phagocytosed than resting spores[62]. In some species, this is linked to spore size, with larger spores (12.3 μm) less readily phagocytosed than small spores (4.3 μm)[27]. However *R. microsporus* spores are on average 5 μm[68]. Finally, in addition to evading uptake, engulfed Mucorales can survive within the phagolysosome via a mechanism that, at least in part, involves melanin-mediated phagosome maturation arrest through inhibition of LC3[40,41,69-71].

Here, we investigate the interaction of host immune cells with *R. microsporus* during the earliest stages of infection and report for the first time a role for a bacterial endosymbiont of *R. microsporus* in disease in both zebrafish and murine models of infection. Specifically, we observed a significant reduction in phagocytosis of metabolically activated spores compared to resting spores. Further *in vivo* and *in vitro* investigation revealed the bacterial endosymbiont to be the producer of an antagonistic compound with anti-phagocytic activity, which we term Phagocin R. In a companion paper, Sephton-Clark et al. investigate the impact of endosymbiont status on fungal and macrophage transcriptional profiles, revealing altered macrophage polarization in response to wild type vs cured *R. microsporus* spores.[72] Here we investigate the consequences of endosymbiont status on infection outcome and demonstrate that this bacterial endosymbiont contributes to both fungal stress resistance and immune evasion during the earliest stages of infection, enabling fungal pathogenesis.

RESULTS

Resting spores are readily phagocytosed, yet swollen metabolically active spores inhibit macrophage functions

We previously showed that the early stages of host-fungus interaction determine disease outcome in the zebrafish model of mucormycosis[41]. Our data suggest that successful control requires both 1) the presence of phagocytes at the site of infection within the first 24 hours and 2) the formation of a granuloma capable of killing spores. We hypothesized that, in instances where infection control fails, spores might evade phagocytosis. In the case of *Aspergillus*, dormant spores are encased in a rodlet layer (RodA) that masks key cell wall PAMPs[17,67]. This layer is shed when spores swell and germinate, providing an opportunity for phagocyte detection. There is no evidence of hydrophobins similar to RodA in the mucormycete lineage[73], however resting and swollen *Rhizopus* spores demonstrate limited immunogenicity[62]. We hypothesized that masking of the spore surface might allow *R. microsporus* spores to evade host detection.

To test this hypothesis, we directly compared uptake of dormant and swollen spores from *R. microsporus* FP469, a clinical isolate from a patient at the Queen Elizabeth Hospital, Birmingham. While dormant *Rhizopus* spores were readily engulfed by J774A.1 macrophage-like cells, swollen, metabolically active *Rhizopus* spores were engulfed at significantly lower rates ($p>0.0001$) (**Figure 1a**). Reduced spore uptake compared to *Aspergillus* was previously reported for *R. oryzae*, with the suggestion that increased spore size might explain the difference[74]. However, in our hands phagocytes were equally able to take up 12 μm particles, which are larger than swollen spores (which reached a mean diameter of 7.3 μm after 6 hours) (**Supplemental S1 Table** and **Supplemental S2a Figure**). UV treatment of washed, pre-swollen spores restored their phagocytosis by J774A.1 macrophages (**Supplemental S2b Figure**). Although total chitin (CFW, Median Fluorescence Intensity) increased more than 2-fold upon swelling (**Figure 1b**), we observed no alteration in surface exposure for chitin (WGA) or total protein (FITC) between resting and swollen spores (**Supplemental Figure S3**). There was no detectable β-glucan exposure, consistent with previous reports showing a lack of glucan in *Rhizopus* species spore cell walls (**Supplemental Figure S4a**).[33,75] Consistent with dynamic cell wall remodeling observed in other fungi, we did observe changes in the key PAMP mannan: compared to resting spores (47.3%) there was a small but reproducible increase in the proportion of cells with high mannan exposure after 2 hours (59.3%) that declined after 4 hours (52.3%) (**Figure 1b**). However, remodeling did not correlate with the observed downward trends in phagocytosis.

Together, these findings suggested active fungal evasion of host phagocytic cells upon germination via a previously undescribed mechanism. To investigate immune evasion by swelling spores, we allowed *Rhizopus* spores to swell in macrophage medium (sfDMEM) for 1 hr and tested the capacity of this supernatant to inhibit phagocytosis of other particles. This supernatant was sufficient to inhibit phagocytosis of dormant spores, demonstrating a trans-protective effect **(Figure 1c)**. Swollen spores from a range of mucormycete genera and species, including *Mucor circinelloides*, *Lichtheimia corymbifera*, and *Cunninghamnella bertholletiae*, were also less readily phagocytosed, and their swollen spore supernatants had a similar protective effect on phagocytosis of resting *R. microsporus* spores (**Figure 1d, e*).*** Supernatant from *R. microsporus* and several, but not all, of the other isolates also had a cross-protective effect on non-mucormycetes, inhibiting phagocytosis of the ascomycete yeasts *Candida albicans* and *Saccharomyces cerevisiae* (**Figure 1f**). These results suggest that species spanning the Mucormycota secrete compounds with broad anti-phagocytic effects. As *R. microsporus* exhibited the strongest effect, we focused on this isolate for the

remainder of the work.

Fungal supernatant of *R. microsporus* can inhibit macrophage functions

To further investigate the influence of *R. microsporus* supernatant on immune evasion, we asked what other effector functions of macrophages were affected by *R. microsporus* swollen spore supernatant. First, we assayed macrophage-mediated killing. Resting or swollen spores were co-incubated with J774A.1 macrophage-like cells, un-engulfed spores washed away, macrophages lysed, and spores tested for viability. Consistent with our previous observations and others,[40,41] macrophages did not kill phagocytosed dormant or swollen spores (**Figure 2a)**. Further, macrophages showed a defect in phagosome acidification as measured by lysotracker staining following uptake of both live resting and pre-swollen spores, suggesting a defect in phagosome maturation (**Figure 2b**).[76] Lysotracker staining was significantly reduced following exposure to supernatant alone (**Supplemental Figure S5a**). Phagosome maturation was significantly improved for uptake of UV killed spores ($p<0.0001$), suggesting that inhibition of macrophage function is an active process (**Figure 2b**). We also noticed that supernatant treatment affected macrophage morphology: treated cells appeared significantly more rounded than control cells (**Figure 2ci, ii, iii**), suggesting defects in cytoskeletal organization. Actin and β-tubulin polymerization are instrumental for phagocytosis and phagosome maturation.[77] When we examined actin filaments (phalloidin) and microtubules (β-tubulin), we observed a significant reduction in signal intensity in treated vs. untreated macrophages (**Figures 2di, ii, iii and 2ei, ii, iii**). Reduced staining is indicative of profound defects in both actin and β-tubulin polymerisation.[77] Supernatant treatment did not impact overall macrophage viability, as measured by lactate dehydrogenase and trypan blue assays **(Supplementary Figures S5b and S5c).** Together, these data suggest that swollen spores actively secrete a factor with specific anti-phagocytic, but not cytotoxic, activity.

R. microsporus FP469 harbours a bacterial endosymbiont

Mucorales species are widely associated with bacterial endosymbionts.[35,78] The endosymbiont *Burkholderia rhizoxinia* augments fungal pathogenesis of *R. microsporus* in rice seedlings by producing the secondary metabolite Rhizoxin, a toxin that targets a conserved residue in β-tubulin, preventing polymerization.[59,79-81] However, no involvement for endosymbionts in mammalian disease have been reported, either as a requirement for pathogenesis in humans or associated with disease severity in diabetic mice.[35,78] To test the hypothesis that an endosymbiont bacterial product might influence phagocytosis, we first tested for the presence of bacterial endosymbiont 16S rRNA in our *Rhizopus* strain, *R. microsporus* FP469, by PCR (**Figure 3a**). *R. microsporus* FP469 was positive for 16S rRNA (lane 1), which was lost upon treatment of the fungus with the antibacterial Ciprofloxacin (lane 2). PCR for 16S rRNA from WT (lane 4) and cured (lane 5) *R. microsporus* CBS631.82, previously shown to harbor a *Burkholderia* spp. endosymbiont, served as a positive control[59,82]. Through enzymatic and physical disruption of the fungal cell wall, we were able to isolate endosymbionts from FP469 and CBS631.82, and 16S rRNA could be amplified from the isolated bacteria (lane 3,6). Moreover, the endosymbiont could be visualized inside *R. microsporus* FP469 hyphae using the bacterial specific fluorescent marker SYTO 9 (**Figure 3b**). Treatment with Ciprofloxacin was sufficient to visually clear the endosymbiont (**Figure 3b**). We additionally tested for the presence of endosymbiont 16S rRNA in a variety of mucorales strains, including *R. delemar, R. chinensis, L. corymbifera, C. bartholletiae, M. circinelloides f. lusitanicus* CBS-277490, and *M. circinelloides f. lusitanicus* NRRL-3631 (**Figure 3c**). We found evidence of endosymbionts in each isolate,

which could be cured by treatment with Ciprofloxacin. For the remainder of this work, unless otherwise stated, spores treated with Ciprofloxacin were germinated, passaged through sporulation twice, and frozen down for stocks before use as cured spores to limit the possibility that the drug was effecting outcomes.

Ralstonia pickettii mediates fungal stress resistance and survival within macrophages

We examined whether the presence of the bacterial endosymbiont was necessary for inhibition of fungal spore uptake by macrophages. Uptake of cured swollen spores was significantly higher than that of the uncured parent ($p<0.0001$) (**Figure 4a**). To further characterise the endosymbiont, we performed whole genome sequencing of the endosymbiont isolated from *R. microsporus* FP469, which was identified as *Ralstonia pickettii*, a relative of *Burkholderia* commonly associated with soil and water and occasionally associated with contaminated medical equipment as an opportunistic pathogen[83-86]. Supernatant from *R. pickettii* grown directly in DMEM moderately inhibited uptake of resting fungal spores by macrophages, and similar inhibitory activity was observed for the endosymbiont isolated from the *R. microsporus* reference isolate (CBS631.82) ($p<0.0001$; **Figure 4b**). Although both were more inhibitory than supernatant from the cured fungus ($p<0.001$), neither were as inhibitory as the parent fungal strain harboring the endosymbiont ($p<0.0001$). We therefore investigated whether *R. microsporus* augments the pathogenicity of *R. pickettii.* The supernatant inhibitory effect of *R. pickettii* on resting fungal spore uptake was moderately amplified ($p=0.019$) by prior growth (1 hr) in the presence of cured swollen fungal spores, but not with cured fungal mycelium (**Figure 4c**). Co-culture of the bacteria with heat-killed cured fungal spores or mycelium was not protective (**Figure 4c**). These data suggest that the *R. pickettii* is the primary source of the inhibitory factor, and that live fungal spores but not hyphae may provide either a pre-cursor or substrate for factor synthesis or an additional anti-phagocytic factor.

In addition to being necessary and sufficient for the observed reduction in phagocytosis, the endosymbiont also influenced phagosome maturation and cytoskeletal organisation. The inhibitory effect on phagosome maturation observed for fungal spores (**Figure 2b**) was lost in supernatant from endosymbiont free spores (**Figure 4di**), and supernatant from *R. pickettii* was sufficient to inhibit phagosome maturation ($P<0.0001$). Actin and β-tubulin polymerization were likewise influenced by the presence but not the absence of the endosymbiont (**Figures 4dii and diii**).

Finally, we tested the impact of endosymbiont elimination on spore killing by macrophages (**Figure 5Ai**). Spores were co-incubated with J774A.1 macrophage-like cells for 6 or 24 hours and assessed for viability by CFU. The endosymbiont conferred significant resistance to macrophage killing within 6 hours, and this extended to 24 hours ($p<0.0001$). Examination of swollen spores by TEM revealed differences in electron density and width of the interior of the cell wall between endosymbiont-harboring vs. cured spores (**Figure 5b**), suggesting the endosymbiont influences spore cell wall organization. Analysis of changes in the cured spore wall during swelling revealed an increase in total protein (FITC) and exposed chitin (WGA) after 4 hours compared to resting spores (**Figure 5c**), whereas these PAMPs were static in wildtype spores (**Supplemental Figure S4**). Similar to WT spores, there was a transient increase in mannan (ConA) at 2 hours ($p<0.0001$). Consistent with this, compared to wild type spores, cured resting (**Figure 5aii**) and swollen (**Figure 5aiii**) spores were significantly more sensitive to treatment with the host-relevant stresses 0.01% SDS, 5 mM $NaNO_3$, or 1 mM H_2O_2, as well as treatment with the front-line antifungal Amphotercin B

(0.5 μg/ml).

Metabolically activated spores of *R. microsporus* secrete compounds that antagonize effector functions of macrophages

Having identified conditions that stimulate secreted anti-phagocytic activity, we set out to further characterize this factor. Activity was not inhibited by treatment with Proteinase K or sodium periodate, and was resistant to boiling, suggesting that the potential inhibitory compounds are not a carbohydrate or protein (**Supplemental Figure S6a**). To further investigate this, we performed a chloroform extraction of the supernatant and confirmed the anti-phagocytic activity of this extract (**Supplemental Figure S6b**). The chloroform extract was further fractionated by HPLC to identify active peaks with anti-phagocytic activity (**Figure 6a**). HPLC analysis revealed clear differences between this chloroform extract (**Figure 6a,** black bars) and a chloroform extract of DMEM alone (**Figure 6a,** grey bars). Relevant HPLC peaks were isolated and their inhibitory activity tested, with peaks 3, 5 and 8 (as annotated in **Figure 6a**) showing significant inhibitory activity (**Figure 6b**). Treatment of spores with Ciprofloxacin abolished all active HPLC peaks in supernatant from cured spores (**Figure 6c**). However, consistent with reduced inhibitory activity of the bacterial supernatant alone (**Figure 4b)**, HPLC analysis of supernatant from monoculture of the bacteria alone recovered only two (3 and 8) of the three active peaks found in the untreated endosymbiont-harboring fungal supernatant (**Figure 6c**).

To identify compounds contributing to the inhibitory activity of the isolated peaks, we analysed the composition of each peak using mass spectrometry. Peak 5 contained several masses of interest, including 696.82, 421.29, 319.42, and 251.34 *m/z*. Peak 8 and Peak 3 contained smaller fragments, including 329.26, 291.40, 203.90, 161.31, 130.31 and 194.12, 163.24, 162.31, 144.28 *m/z*. The identified peaks did not include Rhizoxin (626.59 *m/z*) or the related compound Rhizonin (834.5 *m/z*) (**Supplementary Figure S7**), potent toxins produced by bacterial endosymbionts of the *Burkholderia* spp. that were originally identified in the secretomes of mucormycetes.[59,60] In HPLC analyses, a Rhizoxin control eluted much later than the three active peaks (**Figure 6c**). In addition, compared to bacterial supernatant, Rhizoxin-treated cells demonstrated significantly more inhibition of phagocytosis ($p<0.0001$) (**Figure 6d**) and reduced actin polarization ($p<0.0001$) (**Figure 7a**), but similar activity against β-tubulin (**Figure 7b**), suggesting differences in mode of action and specificity. Together, these results suggest that the target compound produced by *R. pickettii* is not a known Rhizoxin derivative.

The host-relevant medium DMEM is a nutrient-poor medium for bacterial and fungal culture and supports limited growth. We therefore asked whether other nutrient-rich media would support expression of peak 5, the most active peak. HL-5 is a common medium for the cultivation of the mini-host *Dictyostelium discoideum*, a model system for amoebae that are natural predators of fungi [87-89]. Incubation of *R. pickettii* in HL-5 produced a profile consistent with peaks 3 and 5 as well as a number of novel peaks not observed in DMEM. Several of these peaks were lost in HL-5 alone (**Figure 6e**). Neither peak was observed when *R. pickettii* was incubated in VK medium, previously used to induce the expression of Rhizoxin [59].

Burkholderia spp. have been shown to produce a variety of Rhizoxin and Rhizonin derivatives[90] via a *trans*-Acyl Transferase Non-Ribosomal Peptide Synthase Polyketide Synthase (*trans*-AT NRPS PKS) secondary metabolite cluster. Analysis of our *R. pickettii* isolate genome using antiSMASH (5 beta) software for secondary metabolite clusters did not

identify a *trans*-AT PKS.[91] However it did reveal a Type I Polyketide Synthase (Type I PKS), as well as siderophore, bacteriocin, terpene, and arylpolyene, among others. The Type I PKS encoded all expected modules required for function including acyl carrier protein (APC), acyltransferase (AT), ketosynthase (KS), ketoreductase (KD), dehydratase (DH) and enoyl reductase (ER). RNAseq of *R. pickettii* grown in VK medium or DMEM alone (negative conditions) vs HL-5 or DMEM + Fungal substrate (positive conditions) revealed only three upregulated transcripts: the Type I PKS, a predicted NapD-type chaperone, and putative a copper-ATP ABC transporter (**Figure 6f**).

Based on the differences in MS profile, HPLC elution, biological activity, and predicted synthesis pathways, we conclude that this data reveal a previously undescribed compound and here name this compound Phagocin R pending its further identification. Future work will characterize the specific biosynthetic pathways responsible for synthesis of Phagocin R.

Bacterial fungal symbiosis enables fungal survival *in vivo*

Finally, we investigated the influence of bacterial-fungal symbiosis in Mucorales pathogenesis *in vivo*. Our *in vitro* data suggest that the endosymbiont mediates immune evasion during the early stages of germination by preventing phagocytosis, phagolysosome maturation, and killing. To model this *in vivo*, we moved to the zebrafish (*Danio rerio*) larval model of infection (**Figure 8a**). Wild-type embryos (n=30 per group) were infected with either resting or swollen wild type or cured spores and observed for survival (**Supplemental Figure S9aB**). There was a significant difference in fish survival following infection with wild type versus cured spores using either resting ($p=0.019$) or swollen ($p<0.0001$) spores (**Figure 8a**). Notably, survival of fish injected with either resting or swollen cured spores was not statistically different from mock injection in this model ($p > 0.05$). This correlated with CFUs over time: While no differences were observed in initial inocula, within two hours of injection cured spores showed significantly reduced CFUs in zebrafish (n=15 per group, $p<0.0001$) **(Figure 8b**). Over the course of 96 hours, cured spores were more rapidly cleared from infected fish compared to wildtype spores ($p<0.0001$) **(Figure 8b)**, and resting spores were more rapidly cleared than pre-swollen spores (**Supplemental Figure S8a**). Together, these data suggest that the endosymbiont may aid immune evasion during the initial phase of infection, and that the transition from resting to swollen spore is important for this process.

We previously demonstrated that factors that influence the peak number of phagocytes at the site of infection (carrying capacity) in the first 24 hours correlate with disease outcome, and that successful infection control requires spore killing[41]. To investigate the role of the endosymbiont in modulating host defense, we measured phagocyte recruitment in transgenic zebrafish, which enables direct visualization of macrophages and neutrophils to the site of infection (Supplemental Figure S9)[64]. Zebrafish expressing either fluorescent macrophages (Tg(mpeg1:G/U:NfsB-mCherry) (**Supplemental Figure S9b**) or neutrophils (Tg(mpx:GFP)^{i114}) (**Supplemental Figure S9c**) (n=4; means of 4 biological replicate experiments with 3 fish each) were infected with cured or wild-type resting spores and then the number of phagocytes recruited to the site of infection was followed for up to 96 hours (for survival curves, see **Supplemental Figure S8b**).[92,93]

Overall, there were significant differences in the absolute number of macrophages recruited to the site of infection across the different conditions (**Supplemental Figure 8c**). For fish infected with cured resting spores, within the first 24 hours there were significantly more macrophages recruited to the site of infection than for wildtype resting spores (**Figure 8ci**) ($p<0.0001$), and there were significantly more macrophages maintained at the site of

infection after 48 hours in these fish ($p<0.0001$) (**Figure 8cii**). Similar patterns were observed for neutrophil recruitment (Figure 8di, ii, Supplemental Figure 8d).

These data are consistent with established reports that phagocyte activity is a key determinate of survival in mucormycosis. Fish that failed to recruit macrophages after 24 hours regardless of endosymbiont status did not survive until the end of the assay. However, recruitment of macrophages to the site of infection was protective when the endosymbiont was absent, consistent with a role for the endosymbiont in resistance to macrophage-mediated infection control.

Next, we attempted to model the impact of antibiotic treatment immediately prior to or during infection on disease outcome. Concomitant treatment of fish with 60 μg/mL Ciprofloxacin had no effect on fish survival or spore CFU upon infection with either resting or swollen spores (**Supplemental figure S8e**). Therefore, we instead performed a small pilot study in immune-competent mice (n=5 per group**).** Mice were infected intra-tracheally with resting spores that had been untreated or treated with Ciprofloxacin for 3 hours immediately prior to inoculation. CFUs were measured after 4 and 48 hours. Similar to the rapid spore killing observed in fish (Figure 8b), after 4 hours, there was a reduction in CFUs recovered from mouse lungs for the ciprofloxacin treated resting spores ($p=0.019$) (**Figure 8e**). We ruled out a direct inhibitory effect of Ciprofloxacin on fungal survival as swollen spores treated with Ciprofloxacin were as resistant to host killing as untreated swollen spores ($p=0.095$) (**Supplemental Figure S8f**). After 48 hours, there was a significant difference between mice infected with Ciprofloxacin-treated and untreated resting spores ($p=0.0384$, Chi-square test, Newcombe/Wilson with continuity correction), with 60% attributable risk (**Figure 8f**). This effect was lost when mice were infected with swollen spores (**Supplemental Figure S8g**)

Overall, our findings point to a role for the bacterial endosymbiont in fungal immune evasion during early infection via a novel secreted factor that can modulate the macrophage-mediated antifungal response by impacting macrophage-mediated killing, influencing immune cell recruitment, and supporting host-relevant mechanisms of fungal stress resistance.

Discussion

In this work, we demonstrate that the human fungal pathogen *Rhizopus microsporus* harbors a bacterial endosymbiont capable of influencing fungal interaction with mammalian phagocytes and modulating fungal virulence. Our findings highlight an emerging theme in fungal pathogenesis that urges a broader view of fungal growth and virulence to encompass cross-kingdom interactions reflecting the ecological origins of infecting species. A wide diversity of fungi harbor bacterial endosymbionts that influence fungal phenotypes related to growth, sporulation, and pathogenesis in plants.[94-98] Here we report for the first time a role for a bacterial endosymbiont in animals during infection with *R. microsporus*, a prevalent causative agent of fatal mucormycosis.

Fungi harbor a wide diversity of bacterial endosymbionts that are specifically adapted to colonize their fungal hosts and significantly influence host-relevant fungal phenotypes, including metabolism, cell wall organization, development, and plant host colonization[35,58,59,81,90,94,96-106]. Additionally, endobacteria are a source of potent mycotoxins that can influence fungal pathogenesis in plants and insects[59,60,81,90,107,108]. New patient populations are now susceptible to a broadening diversity of basal saprobic fungi, which are a major emerging cause of clinically important superficial and disseminated fungal

infections[18,109]. However, the role of endosymbionts in pathogenesis during mammalian mucormycosis has yet to be clinically defined, representing a significant gap in our understanding of the pathogenicity of mucormycetes.

In this study employing several lines of evidence, we report that a clinical isolate of *R. microsporus* harbors a bacterial endosymbiont that influences host–pathogen interactions. We show that during the early steps of spore germination the bacterium secretes a factor that inhibits phagocytosis. In addition, *R. microsporus* spore survival following phagocytosis by macrophages is dependent on the presence of the endobacterium. Elimination of the bacterial endosymbiont by ciprofloxin treatment facilitates macrophage killing and *in vivo* clearance of fungal spores.

While previous work has focused on *Burkhoderia-Rhizopus* endosymbiosis, we identify a previously unappreciated niche for the related gram-negative bacterium *Ralstonia pickettii* as an endosymbiont of *R. microsporus.* Consistent with long-term mutualism, we observed an overall reduction in RNS/ROS stress resistance and virulence in a cured *R. microsporus* isolate. We also observed reduced sporulation and overall fitness in this strain after repeated passage of fungal growth on SDA plates with cirpofloxacin. Mondo *et al.*, showed that bacterial endosymbionts can impact fungal sporulation and development through controlling *ras2*, a key GTPase that regulates fungal sexual reproduction[58]. In our companion work examining the response of *Rhizopus microsporus* to the presence of the endosymbiont_we observed very few changes at the transcriptional level during growth in DMEM. Specifically, loss of the endosymbiont was associated with reduced expression of a gene implicated in autophagy.[72] Fungal autophagy has been shown to influence lipid biogenesis, morphogenesis, development, and virulence.[110] Consistent with a change in lipid biogenesis, we observe changes in the fungal plasma membrane in cured spores, as well as increased sensitivity to Amphotercin B, indicative of altered ergosterol content. Loss of the endosymbiont had profound impacts on *R. microsporus* response to phagocytosis, leading to altered regulation of 359 genes, including inappropriate repression of genes involved in siderophore activity and iron scavenging.[72] We observed a similar global change in the intensity of the fungal response to phagocytosis in a cured isolate of *R. delemar* lacking an unculturable endosymbiont with high 16S sequence homology to other unculturable bacteria (Accession number MK573034).[72] Together, our findings support a mutualistic lifestyle for *R. pickettii* and *R. microsporus*.

In addition to supporting fungal development and stress resistance, we show that *R. pickettii* inhibits phagocytosis by macrophages during the initial steps of germination. We demonstrate that this is facilitated by the production of a unique bacterial factor, which we name Phagocin R. We further note that phagocin R exhibits several anti-phagocytic effects including impacting mammalian cell morphology and cytoskeleton organisation, particularly actin and β-tubulin polymerization as well as phagosome maturation. These findings add to reports of bacterial endosymbionts that facilitate pathogenesis, first revealed by the finding that *B. Rhizoxina* increases *R. microsporus* pathogenesis through production of the phytotoxin Rhizoxin, an antimitotic agent that targets the cytoskeleton[107]. Phagocin R appears to be distinct from Rhizoxin in activity (**Figure 7**) and biosynthesis, as evidenced by analysis of secondary metabolite clusters in the *R. pickettii* genome. Further, we show that the presence of the endosymbiont reduces fungal sensitivity to host phagocyte antimicrobial activity and that this can have implications for pathogenesis during the earliest stages of mammalian infection.

Two groups recently reported that although bacterial enodsymbionts, including Rhizoxin and Rhizonin producers, are widely found among mucormycete clinical isolates, these endosymbionts did not impact pathogenesis during mucormycosis in both mouse and fly models[35,78]. The influence of endosymbiont-derived Rhizoxin on pathogenesis was assessed in a diabetic mouse model[35]. Diabetic mice were infected with *Rhizopus* isolates harboring Rhizoxin-producing *Burkholderia* endosymbionts and then treated with either Amphotericin B antifungal or Ciprofloxacin antibacterial or both 24 hours post-infection. No impact for Ciprofloxacin treatment was observed in that work[35]. In contrast, in our work, when immune-competent mice were infected with resting spores pre-treated with Ciprofloxacin, CFUs were reduced compared to untreated within 4 hours and spores could no longer be recovered after 48 hours. It should be noted that the work here was performed in a small number of mice (5 per group) and therefore is prone to the challenges associated with underpowered models of infection. We observed similar patterns in the zebrafish model of infection, which simultaneously allows larger study populations and detailed dissection of mechanisms of innate immune defense. We again observed a profound improvement in zebrafish larval survival upon infection with spores lacking the endosymbiont. In both models, the endosymbiont appears to play a more significant role during the transition from resting to swollen spore, however direct infection with swollen cured spores was still associated with reduced host death. We hypothesize that in our model, the elimination of the endobacterium restores robust phagocyte recruitment and promotes macrophage killing of fungal spores, factors that remain defective in the diabetic or immune-suppressed host models.

During *in vivo* infection of immunocompetent mice, the closely related fungus *R. oryzae* was shown to be phagocytosed but not killed by alveolar macrophages, while unengulfed spores were associated with neutrophil recruitment.[40] Swollen spore survival was linked to resistance to iron limitation and melanin-mediated arrest of phagosome maturation. These findings are consistent with observations in zebrafish showing the formation an early granuloma comprised of macrophages and neutrophils in response to *M. circinelloidei* that likewise controlled but failed to kill spores and suggest a similar host response to a variety of infecting Mucorales species.[41,64] Spore survival within macrophages *in vitro* and within early granuloma in immunocompetent mice indicate a potential reservoir for latent fungal infection. Indeed, an emerging trend in clinical reports of mucormycosis is the unappreciated burden of indolent or chronic mucormycosis.[39] The observation that elimination of bacterial endosymbionts impacts cell wall organization, resistance to host relevant stress, and resistance to macrophage-mediated killing raises the possibility that modulation of fungal endosymbiont status may impact fungal latency and allow clearance.

Together, our findings highlight the importance of bacterial symbiosis in the pathogenesis of mucormycosis. However, we urge caution in extending our findings to all Mucorales or fungal endosymbionts. While a number of studies have demonstrated general features common to host-Mucorales interactions, there may be species-specific aspects that influence Mucorales pathogenesis. In addition, not all clinical isolates profiled harbor endosymbionts, suggesting that endosymbionts may augment, but are not constitutively required for, pathogenesis[35]. Overall, our findings point to a role for the bacterial endosymbiont in fungal immune evasion during infection via a secreted factor and raise the possibility of a role in reactivation of latent infections with resting spores in patients undergoing immunosuppressive therapy[111]. Harnesing the role of bacterial symbiosis could prove key in revolutionalising mucormycotic management through combination therapy of anifungal and antibiotics.

Methods

Media and growth conditions. Fungal strains were routinely cultured on Sabouraud dextrose agar (SDA) (EMD Millipore co-operation) or potato dextrose agar (PDA) to induce sporulation at room temperature. Routine liquid cultivation was performed in 500 mL conical flasks containing 250 mL of serum free Dulbecco's modified eagle's media (with 1% penicillin/streptomycin and L-glutamine) (DMEM). Fungi grown in this way was used for metabolic activation of spores, to prepare swollen spore supernatants, and for DNA isolation. For bacterial isolation, fungi were fermented in 250 mL flasks containing VK media (1% corn starch, 0.5% glycerol, 1% gluten meal, 1% dried yeast, 1% corn steep liquor, 1% $CaCO_3$) and pH adjusted to 6.5, as previously described by [90]. The bacterial isolates were grown on nutrient agar plates at 30°C. All chemicals for media, buffers, and supplements were purchased from Sigma Aldrich unless otherwise indicated.

Macrophage cell line culture. J774A.1 murine macrophage-like cells were maintained in DMEM supplemented with 10% foetal bovine serum, 1% Streptomycin (100 µg/mL), penicillin (100 U/mL), and 1% L-glutamine (2 mM). The cells were cultivated in a humidified environment at 37°C enriched with 5% CO_2 and used between 3 and 15 passages after thawing.

Sporangiospore harvest and preparation. Mucormycetes sporangiospores generated from hyphae for 14-24 days were harvested by flooding the surface of the culture plate with 10 mL of PBS, washed 3x, and counted with a haemocytometer. Spores were used within 14-24 days of sporulation as previously described by [64]. Spores prepared in this way are defined as "resting spores". For experiments that required metabolically active spores, incubated in Sabouraud broth media or serum free DMEM media at 37°C with shaking at 200 rpm for 4 h, collected by centrifugation, and washed with 1xPBS. Spores prepared this way are defined here as pre-germinating, swollen or metabolically active spores. For experiments requiring UV killed spores, resting or swollen spores were suspended in 20 mL 1xPBS, irradiated twice for 15 min in a UV PCL-crosslinker at 1200 µJ/cm^2, and cooled on ice between treatments as previously described by [64]. Successful killing was confirmed by plating for CFUs. **Latex beads** were also processed similarly to spores including washing with PBS, counting and re-suspension.

Stress resistance of spores. Mucormycete spores (parent or cured) were tested for susceptibility towards a range of stress conditions. The settings mimicked different degrees of oxidative (0.25, 0.5, 1, and 5 mM hydrogen oxide (H_2O_2)), Nitrosative (1, 5, and 20 mM sodium nitrite ($NaNO_2$) (Fisher scientific)), cell wall (0.005, 0.01, 0.05% sodium dodecyl sulphate (SDS) (Fisher scientific)), osmotic (0.05, 0.1, 0.3 M sodium chloride (NaCl)) (Sigma-Aldrich) and antifungal pressure (0.5, 1, 2.5, 5 µg / mL Amphotericin B (AmB) (Sigma Aldrich) stress. The spores were counted and adjusted to 10^5 cells /mL in *sf* DMEM containing the stress factor at the respective concentrations in a 48 well plate, and incubated at 37° C and 5% CO_2 for 24 h. To evaluate the influence of the stress factor on the spores, serial dilutions were plated and colony forming units (CFUs) counted after 24 h (parent) or 48 h (cured) spores.

Microscopy

Fluorescent staining of spores. For experiments requiring stained spores, the spores were counted, adjusted to $2x10^7$/ml in PBS and stained with 100 μg/mL fluorescein isothiocynate isomer 1 (FITC) (Sigma-Aldrich) in 0.1 M sodium bicarbonate buffer (pH 7.45) (Sigma Aldrich), 25-50 µg/mL RhTRITC-concanavalin A (ThermoFisher scientific) or 250 µg/ml calcofluor white (Sigma Aldrich) in PBS for 30 min with shaking at room temperature. For flow cytometry, resting *R. microsporus* FP 469-12 spores were pre-germinated at the indicated time points in sfDMEM at 37°C 200 rpm, fixed in 4% methanol-free formaldehyde, and incubated singly with either 0.01 ug/ml Dectin-1 IgG antibody, washed, and 1:200 goat anti-mouse IgG-488 secondary antibody (β-glucan); Calcofluor white (CFW, chitin; 250 µg/ml); or ConcanavalinA (ConA-488; 50 µg/ml). Binding was assessed for at least 10,000 cells using an Attune NxT flow cytometer compared to a pooled secondary-only control. Data are representative of three independent experiments.

Imaging acquisition. For live-cell imaging, J774A.1 macrophage-spore co-cultures were maintained in sfDMEM+ 50 nm LysoTracker Red DND-99 (Invitrogen, molecular probes) under humidified conditions at 37°C with 5% CO2 for the indicated period of time. Live-cell timelapse images were acquired under phase contrast at 14X magnification on a Nikon Ti microscope (20x magnification combined with a 0.7x de-magnifier) equipped with a QICAM Fast 1394 CCD camera (QImaging). Fixed-cell fluorescence imaging was, unless stated otherwise, performed at 63x magnification on a Zeiss Axio Observer Z1 equipped with structured illumination (Apotome) using a Flash 4 sCMOS camera (Hamamatsu).

Image processing. Image processing and analysis was carried out using either ImageJ or Metamorph software.

TEM *R. microsporus* spores were collected and allowed to swell as described above. Samples were processed via high-pressure freezing using a Bal-Tec HPM 010 high-pressure freezer (Boeckler Instruments, Tucson, AZ) and then transferred to an RMC FS-7500 freeze substitution unit (Boeckler Instruments, Tucson, AZ). Samples were freeze substituted in 2% osmium tetroxide, 1% uranyl acetate, 1% methanol, and 5% water in acetone, then transitioned from −90°C to room temperature over 2 to 3 days, rinsed in acetone, and embedded in LX112 epoxy resin (Ladd Inc., Burlington, VT). Ultrathin sections of 70 to 80 nm were cut on a Leica Ultracut UC7 microtome, stained with uranyl acetate followed by lead citrate, and viewed on a JEOL 1200EX transmission electron microscope at 80 kV.

Supernatant collection. Sporangiospores were harvested as described previously[64], counted and adjusted to $4x10^8$ spores/mL in 250 mL of serum free DMEM with or without 60 µg/mL Ciprofloxacin, and incubated at 37°C with shaking at 200 rpm for 4 h. Following incubation, the supernatant was centrifuged at 3990 rpm for 5 mins and filter sterilised through a 0.45 µm filter. For inactivation experiments, the supernatant was boiled at 100°C for 1 h, digested with 50 µg/mL proteinase K at 37°C for 1 h and oxidised with 1 nmoles/ml of sodium periodate ($NaIO_4$) at 37°C with mild shaking for 45 min. For size exclusion, 15 mL of supernatant was filtered through an Amicon® tube (Sigma-Aldrich cat number UFC801024) equipped with a 3 kDa ultra-centrifugal filter. Samples were centrifuged for 30 min at 3000 g and both the 'flow through' (*i.e.* fitrate) and 'concentrated portions of the supernatant' (*i.e.* retained by the filter) were kept for phenotypic analysis.

Phagocytosis assay. One day prior to the experiment, 1 mL of 10^5 cells/mL J774A.1 murine macrophage-like cells [112] were seeded in a 24 well plate in pre-warmed (37°C) complete Dulbecco's modified eagles' media (cDMEM) supplemented with 5% Foetal bovine serum

(FBS), 1% penicillin/streptomycin and 1% L-glutamine. Incubated at 37°C +5% CO_2 overnight to form a cell monolayer. Following incubation, the overnight media was aspirated, cells washed 2x with pre-warmed PBS, refreshed with 1 mL pre-warmed serum free DMEM (sfDMEM) and incubated at 37°C +5% CO_2 for 1 h. The media was aspirated, cells washed 2x with PBS, and a suspension of FITC pre-stained resting or swollen spores in sfDMEM was added a concentration $5x10^5$ spore/mL for a multiplicity of infection (MOI) of 1:5. The co-culture was incubated 37°C +5% CO_2 for 1 h to allow spore uptake. Phagocytosis was terminated by PFA fixation for 15 min, and washed with PBS prior to counter stained with Concanavalin A (Con-A) or calcoflour white (CFW). Following a 30 min incubation, cells were washed, maintained in PBS and imaged under phase contrast on a Nikon T1 microscope. For experiments requiring use of UV killed or metabolically activated spores, latex beads, *C. albicans* or *S. cerevisiae*, the particles were prepared as described above. For supernatant effect experiments, the cells were treated with 75% supernatant or 3 pmoles/mL Rhizoxin (where indicated) in sfDMEM during co-cultured with indicated spores or particles for 1 h and washed 3x before phagocytosis examination. Uptake rate was quantified as the number of phagocytes containing at least one spore. Statistical differences were determined compared to the indicated control using Student's t-test. For multiple comparisons, statistical significance was assessed using One-way ANOVA and Tukey's test or Two-way ANOVA and Bonferroni's test as indicated in the figure legends.

Macrophage characterization. To assess F-actin and beta tubulin polymerisation, J774A.1 cells were seeded onto round 13 mm coverslips in 24 well plates and cultured as described. Prior to staining, cells were challenged with supernatants or 3 pmoles/mL Rhizoxin and incubated on ice for 10 min. Media was then replaced with pre-warmed sfDMEM and the cells were incubated for 30 min. Samples were then fixed with 4% PFA for 10 min, permeabilised with 0.1% Triton X for 5 min and washed 3x with PBS. To stain for beta tubulin, coverslips were firstly immersed in 1% bovine serum albumin (BSA) for 1 h and further incubated overnight in PBS containing 5 µg/mL anti-beta tubulin ab18207 (Abcam) primary antibody and 0.1% BSA. Samples were then washed and incubated with 2 µg/mL Alexa Fluor 488 goat anti-rabbit secondary ab 150081(Abcam) for 1 h. For f-actin staining, samples were incubated with 3 nanomolar phalloidin conjugated to Alexa Fluor 488 (Thermofisher Scientific) for 15 min. After cytoskeleton staining cells were counter-stained with 2 µg/mL Hoechst (4'6 Diamichino-2-phenylindol for 15 min) where appropriate and mounted onto glass slides with Prolongo antifade mountant (Thermofisher Scientific). Phagosome maturation was assessed as previously described[113]. Briefly, macrophage monolayers prepared as described above were stained with 50 nm LysoTracker Red DND-99 (Invitrogen, molecular probes), pre-treated as described for 1 hour, and co-incubated with killed fungal spores for 2 hr. Cells were imaged and individually assessed for overall fluorescence intensity compared to untreated controls.

Macrophage viability. Lactate Dehydrogenase (LDH) Activity was estimated by measuring the conversion of NAD to NADH by supernatants using a kit according to the manufacturer's instructions (Sigma, MAK066-1KT). Colorometric output was measured using a FLUO-star Omega plate reader at 450 nm and calculations performed as directed by the insert against the standard curve.

Spore viability. Resistance to killing by macrophages was assessed as following phagocytosis at the indicated time points. Macrophages were lysed with 1 mL sterile water and aggressively washed to collect adherent spore cells. The lysate was serially diluted and 5 µL plated out on SDA for CFUs.

Substrate experiment methods. The requirement for fungal stubstrates for endosymbiont activity were assessed using cured fungal substrates pre-grown on SDA, HL5, DMEM and VK medium. Spores or hyphal masses were harvested, washed, disrupted using a bead beater with sterile soil beads (Qiagen) or heat killed by autoclaving, to yield live or heat killed fungal substrates. The respective substrates (~0.1 g) were collected into sterile 50 mL falcon tubes and co-cultured with 20 mL sfDMEM with of bacterial suspension at optical density (OD) 0.2 and incubated at 30°C with shaking (50-80 rpm) for 24 h. After incubation, the tubes were centrifuged, and supernatant collected and filtered before phagocytic assays commenced.

Generation of endosymbiont-free fungal strains. For the generation of endosymbiont-free (cured) fungal strains, the fungi were cultivated and passaged in the presence of Ciprofloxacin at a concentration of 60 µg / mL for a month and maintained on Ciprofloxacin plates for 3 months before endosymbiont was entirely cleared. Cured fungus was then routinely cultured. Absence of the bacteria was routinely confirmed through fluorescence microscopy by SYTO9 staining, and polymerase chain reaction (PCR) amplification of the 1.5 kb band for bacterial 16S rDNA.

Fermentation of *R. microsporus* for bacterial isolation. To a 250-mL conical flask containing 100 mL of VK media, 200-500 spores were added aseptically and incubated at 30^{o}C with shaking at 80 rpm for 2-7 days.

Localization of bacterial endosymbiont by fluorescence microscopy. Mucormycetes spores were fermented as described, a small sample of mycelia pellet aseptically submerged into 200 mL of 0.85% sodium chloride (NaCl) for 1 h, washed 2x in PBS and stained with the Live/Dead BacLight bacterial viability kit (Thermofisher Scientific). The stain solution was prepared with equal volumes of component A (SYTO 9) and component B (propidium iodide). Mycelia were incubated in stain solution for 15 minutes, fixed with 4% PFA, mounted on glass slides and imaged at (insert magnification) under phase contrast on a Zeiss Axio Observer Z1 microscope.

Isolation of bacterial endosymbiont. A small mycelial pellet was aseptically collected from a 2-4 day old liquid fungal culture and submerged into 500 µL of 2000 units/mL Lyticase enzyme (Sigma-Aldrich) in distilled water and incubated at 25^{o}C for 2.5 h. Using mechanical stress (pipetting or vortexing) the mycelia were broken down and subjected to gradient centrifugation at 13200 rpm for 30 mins. Aseptically, 10 µL of the supernatant were plated on nutrient agar and incubated at 30^{o}C until a bacterial or fungal growth was observed. Bacterial colonies were then sub cultured in LB broth and maintained at -80^{o}C.

***R. pickettii* identification and gDNA and RNA Sequencing.** *R. pickettii* isolates were identified by PCR of total gDNA extracts from *R. microsporus* FP469-12.6652333 using the 16S Universal primers CCGATTCGTCGACAACAGAGTTTGATCCTGGCTCAG and CCCGGGATCCAAGCTTACGGCTACCTTGTTACGACTT as previously described[59]. The resulting PCR products were sequenced and used to search NCBI databases to identify best hits for identification. *R. pickettii* was isolated from *R. microsporus* FP469-12.6652333 using established methods.[59] Bacterial genomic DNA was extracted using the DNeasy PowerLyzer Microbial Kit (Qaigen) and sequenced by MicrobesNG (University of Birmingham, UK). The sample was identified by kraken (v1) highly similar to *R. picketti* J12. Secondary metabolite clusters were identified using AntiSmash version 5 beta software[91].

Transcriptional analysis of *R. pickettii* was assessed following growth for 4 h at 30 °C, 80-150 rpm in VK, DMEM, HL5, or DMEM+cured *R. microsporus* hyphae. Triplicate biological replicates were prepared for each condition. RNA was extracted using the modified Qiagen RNA extraction method as described previously[114]. Briefly, TRIzol was used to lyse the samples, which were then either immediately frozen at -20°C and stored for RNA extraction or placed on ice for RNA extraction. After lysis, 0.2 ml of chloroform was added for every 1 ml of TRIzol. Samples were incubated for 3 min, then spun at 12,000 g at 4°C for 15 min. To the aqueous phase, an equal volume of 100% ethanol (EtOH) was added, before the samples were loaded onto RNeasy RNA extraction columns (Qiagen). The manufacturer's instructions were followed from this point onwards. RNA quality was checked by Agilent, with all RNA integrity number (RIN) scores above 7. One microgram of total RNA was used for cDNA library preparation. Library preparation was done in accordance with the NEBNext pipeline, with libraries quality checked by Agilent. Samples were sequenced using the Illumina NextSeq platform; 150-bp paired-end sequencing was employed (2 x 150 bp) (>10 million reads per sample). Sequence files are available upon request. Data was analyzed using Hisat2 (Version 2.0.5), HTSeq (Version 0.10.0) and edgeR (Version 3.16.5).

Chloroform extraction and High-performance liquid chromatography (HPLC) analysis of the supernatant. Swollen spore supernatant or medium controls were exhaustively extracted 3x with chloroform in a 2:1 v/v ratio, the combined organic phase dried over anhydrous sodium sulphate, filtered and evaporated to dryness under reduced pressure. The dried product was reconstituted in 500 µL of dimethyl sulfoxide (DMSO) or serum-free DMEM for HPLC analysis or phagocytosis assay. The superantant and respective controls were separated through a Kinetex® C18-EVO column (Phenomenex®: 5 µm, 100 Å, 250 x 4.60 mm) maintained at 35°C, and chromatograms were recorded by UV-Vis detection at 210 nm. HPLC analysis was performed using mixtures of solvent 'A' (water + 0.1% v/v trifluoroacetic acid) and solvent 'B' (acetonitrile + 0.1% v/v trifluoroacetic acid) as mobile phase with the following method: 3%B isocratic for 10 min, 3-50%B gradient for 30 min, 50%B isocratic for 5 min, 50-3%B gradient for 5 min, and 3% isocratic for 10 min, at a constant flow rate of 1 mL/min.

Isolation of individual HPLC peaks and Mass spectrometry. Significant and reproducible HPLC peaks that appeared in the supernatant and not in the control were collected and submitted for high-resolution mass spectrometry (HMRS) analysis, or concentrated under vacuum at 45°C for 20 min to eliminate acetonitrile/trifluoroacetic acid and freeze dried overnight for phagocytic assays. The freeze-dried products were reconstituted into 200 µL of DMSO, then diluted with DMEM to a final concentration of 1%, and filter sterilised through a 0.45 µm filter for phagocytic assay.

Screening for bacterial endosymbiont. To detect the presence of the bacterial endosymbiont, we employed universal primers as applied elsewhere by [35,60] to amplify the 1.5 Kb band for 16S rDNA from genomic DNA isolated from mucormycetes. DNA was obtained from 10^7 spores in a screw cup with beads and homogenised using a bead beater (Bertin technologies) at speed 6500 for 1 min and DNA extracted with a DNeasy® powerlyzer® microbial kit (Qiagen) following the manufacturer's instructions. The primers specific for 16SrDNA were Forward: 5'CCGAATTCGTCGACAACAGAGTTTGATCCTGGCTCAG3', Reverse; 5'CCCGGGATCCAAGCTTACGGCTACCTTGTTACGACTT 3'. PCR condition using

Phusion kit were 35 cycles, at 95^{o} for 2 min, 60^{o}C for 30s, and 72^{o}C for 1 min for both reactions and products analysed by means of gel electrophoresis.

Virulence assays

Mouse model. Immunocompetent CD-1 20-23g male mice (n=12 per group) were infected intratracheally with 25µl serum-free DMEM containing 10^6 resting or swollen *Rhizopus microsporus* spores (FP469-12.6652333). To mimic the early stages of infection, swollen spores were pre-germinated in serum-free DMEM with or without Ciprofloxicin (60 µg/mL) for up to 3 hrs at 37°C, 200 rpm, sufficient to swell but not form germ tubes. Mice (n=5 per group) were sacrificed by pentobarbital overdose and lungs were collected at two different time points: 4 h or 48 h post infection. At each time point, 5 mice per group were sacrificed. Innoculum was verified via lung CFU from two mice directly after infection. Data were tested for normality using Shapiro-Wilk and analysed using the Mann-Whitney U test. Data are reported as Median with 95% CI.

Murine inoculum. Spores were collected from Sabouraud agar plates via floating in 10 mL of PBS + 0.01% Tween 20, washed once with endotoxin-free PBS and resuspended in serum-free DMEM. Spores were counted using a haemocytometer and normalized to 4x10^7/ml.

Zebrafish cultivation and maintenance. We employed both wild type AB and transgenic zebrafish lines. Specifically, the transgenic line Tg(mpx:GFP)^{i114} expresses green fluorescent protein (GFP) in neutrophils [92]. Macrophage-specific expression of red fluorescent protein mCherry was achieved by crossing Tg(mpeg1:Gal4-FF)^{gl25} with Tg(UAS-E1b:NfsB.mCherry)^{c264}, referred to as Tg(mpeg1:G/U:NfsB-mCherry) [93]. Zebrafish were cultivated and maintained in a recirculating system at the University of Birmingham (BMS) Zebrafish Facility. The Zebrafish were kept under a 14 h-10 h light-dark cycle with water temperature maintained at 28°C. All zebrafish care protocols and experiments were performed in accordance with the UK animals (scientific procedures) act, 1986. Following collection of the eggs, at 40-60 eggs per 25 mL E3 media (plus 0.1% methylene blue and 1 mg/mL 1-phenyl-2- thiourea (PTU)) for 24 h and larvae were incubated at 28°C. PTU at this concentration prevented melanization of the embryos. All media and reagents used was purchased from Sigma Aldrich unless otherwise mentioned.

Spore preparation for injection. Spores were collected in 10 mL of PBS, washed 3x and countered using a haemocytometer. For localization, spores were stained with fluorescent brighter 28 in 0.1 M of $NaHCO_3$ for 30 min. Following staining, the spores were washed 3 times in PBS, counted and adjusted to 10^8 spores/mL in 10% (w/v) polyvinylpyrrolidone-40 (PVP) in PBS with 0.05% phenol red in ddH_2O. PVP was used as a carrier medium with increased density and preventing the fast clogging of microinjection needles.

Hindbrain ventricle injections. The fish were injected in accordance to a protocol by Brothers *et al*., 2011) and zebra fish development assessment in accordance to Kimmel *et al*., 1995[115,116]. The fish were injected at prim-25 stage following manual dechorionation and anesthesia with 160 µg/mL of Tricaine in ddH_2O. The fish were then micro-injected with 2 nL of 10% (PVP) in PBS or *R. microsporus* spore suspension at 10^8 spores/mL (high dose) in PVP through the otic vesicle into the hind brain to achieve an inoculum dose of approximately 50-100 spores per fish. Following injection, the larvae were anesthetized with 160 µg/mL Tricaine in E3 media in a 96 well plate and screened by fluorescence microscopy, using the Zeiss Axiobserver Zi microscope equipped with Aptome system for the presence of spores and only larvae with approximate correct inoculum were selected, transferred to

individual wells of a 24 well plate containing E3 media (plus 0.1% methylene blue ± 60 µg/mL Ciprofloxacin). The fish were monitored over a period of 96 hours post infection (96 h.p.i) for survival and at 96 h.p.i the fish were killed following euthanasia with 1600 µg/mL Tricaine overdose and then in bleach overnight before they were disposed of. Chemicals and media used were purchased from Sigma-Aldrich unless otherwise indicated.

Survival was visualized using Kaplan-Meyer survival analysis and pair-wise statistical significance was tested using Mantel-Cox with Bonferroni's correction for multiple comparisons (5% family-wise significance threshold = 0.025).

Evaluation of spore viability. Following injection, a total of 15 (5 fish per biological repeat) per condition were euthanized with 1600 µg/mL Tricaine. The fish were then homogenised in 100 µL of E3 media containing penicillin- streptomycin (5000 U/mL-5 mg/mL) and gentamicin (10 mg/mL) using pellet pestles and plated out on SDA containing 100 U/mL-100 µg/mL penicillin-streptomycin and 30 µg/mL gentamicin. The plates were then incubated at room temperature for between 24 and 48 h and colony forming units (CFUs) examined.

Phagocyte recruitment. To quantify phagocyte recruitment into the hindbrain, transgenic zebrafish larvae Tg(mpx: GFP)^{i114} expressing green fluorescent protein in neutrophils or Tg(mpeg1:G/U:NfsB-mCherry) with macrophage-specific expression of red fluorescent protein mCherry were injected with high dose viable spores stained with calcofluor white and observed after 6 h.p.i up to 72 h.p.i[92,93]. Positive phagocyte recruitment was defined by accumulation of >10 neutrophils or macrophages to the site of infection. At least 3 biological repeats were performed with 5 fish per condition to give a total of 15 fish per group. 3D volumes of the hindbrain were reconstructed from Structured Illumination Microscopy image stacks acquired on an Axio Observer Z1 microscope equipped with Apotome (Carl Zeiss). Cell numbers were accessed with ImageJ using 3D Objects Counter plugin.

Ethical statement. All maintenance protocols and experiments were performed in accordance to Animals (scientific procedures) Act, 1986 as required by United Kingdom (UK) and European Union (EU). All work was performed under appropriate Biosafety Level 2 conditions (BSL2). All zebrafish care and experimental procedures were conducted according to Home Office legislation and the Animals (Scientific Procedures) Act 1986 (ASPA) under the Home Office project license 40/3681 and personal licenses l13220C2C to Kerstin Voelz and lCDB92D64 to Herbert Itabangi. Mouse studies were approved by the Institutional Animal Care and Use Committee of the Los Angeles Biomedical Research Institute at Harbor-UCLA Medical Center, according to the NIH guidelines for animal housing and care under protocol 11671.

Statistics. All data was analysed in Graphpad Prism 7 using the nonparametric, Mann-Whitney U tests, and log rank tests as indicated in the figure legends and main text. Differences with p value ≤ 0.05 were considered significant.

Acknowledgements. We are grateful to Dr. Deborah Mortiboy of the Queen Elizabeth Hospital Birmingham Trauma Centre for isolation and initial identification of *Rhizopus microsporus* FP469-12.6652333 and to Zoe Reading and Bradley Pollard for their contributions to the work during their research projects in the Voelz lab.

Table 1. **Strains used**

NO.	Name	Strain id	Source
1	*Rhizopus microsporus (wildtype)*	FP469-12.6652333	Clinical isolate, Queen Elizabeth Hospital, Birmingham
2	Cured *Rhizopus microsporus*	(FP469-12.6652333)	This study
3	*Ralstonia pickettii*	Bacteria isolated from (FP469-12.6652333)	This study
4	*Rhizopus microsporus*	CBS 631.82	ATCC-52807
5	Cured *Rhizopus microsporus*	Cured CBS 631.82 strain	This study
6	*Ralstonia pickettii*	Bacteria from CBS 631.82	This study
7	*Rhizopus chinensis*		
8	*Rhizopus delemar* (endosymbiont identified as having homology to unculturable bacterium Accession No. MK573034)	RA 99-880	
9	*Lichtheimia corymbifera*	FP454-9.6002134	
10	*Cunninghamella bertholletiae* (endosymbiont identified as *Sphingomonas wittichii*)	NB2	Obtained from Ashraf Ibrahim (UCLA)
11	*Mucor circinelloides f. lusitanicus* (endosymbiont identified as *Micrococcus luteus*)	FP624-CBS-277490	This study
12	*Mucor circinelloides f. lusitanicus* (endosymbiont identified as *Micrococcus luteus*)	FP623-NRRL-3631	This study
13	Cured *Rhizopus chinensis*		This study
14	Cured *Rhizopus delemar*	RA 99-880	This study
15	Cured *Lichtheimia corymbifera*	FP454-9.6002134	This study
16	Cured *Cunninghamella bertholletiae*	NB2	This study
17	Cured *Mucor circinelloides f. lusitanicus*	FP624-CBS-277490	This study
18	Cured *Mucor circinelloides f. lusitanicus*	FP623-NRRL-3631	This study
19	*Candida albicans*	SC5314	Obtained from Neil Gow
20	*Saccharomyces cerevisiae*	AM13/0001	Obtained from Neil Gow
21	*Burkholderia cepacia*	Clinical isolate from cystic fibrosis patient	Obtained from Queens University Belfast

References

1 Erwig, L. P. & Gow, N. A. Interactions of fungal pathogens with phagocytes. *Nat Rev Microbiol* **14**, 163-176, doi:10.1038/nrmicro.2015.21 (2016).

2 Carrion, S. d. J. *et al.* The RodA hydrophobin on Aspergillus fumigatus spores masks dectin-1- and dectin-2-dependent responses and enhances fungal survival in vivo. *Journal of Immunology (Baltimore, Md : 1950),* **191**, 2581–2588, doi:10.4049/jimmunol.1300748 (2013).

3 Rappleye, C. A., Eissenberg, L. G. & Goldman, W. E. Histoplasma capsulatum alpha-(1,3)-glucan blocks innate immune recognition by the beta-glucan receptor. *Proc Natl Acad Sci U S A* **104**, 1366-1370, doi:10.1073/pnas.0609848104 (2007).

4 Garfoot, A. L., Shen, Q., Wuthrich, M., Klein, B. S. & Rappleye, C. A. The Eng1 beta-Glucanase Enhances Histoplasma Virulence by Reducing beta-Glucan Exposure. *MBio* **7**, e01388-01315, doi:10.1128/mBio.01388-15 (2016).

5 Ballou, E. R. *et al.* Lactate signalling regulates fungal beta-glucan masking and immune evasion. *Nat Microbiol* **2**, 16238, doi:10.1038/nmicrobiol.2016.238 (2016).

6 O'Meara, T. R. & Alspaugh, J. A. The Cryptococcus neoformans capsule: a sword and a shield. *Clin Microbiol Rev* **25**, 387–408, doi:10.1128/CMR.00001-12 (2012).

7 Kronstad, J. W. *et al.* Expanding fungal pathogenesis: Cryptococcus breaks out of the opportunistic box. *Nature reviews Microbiology* **9**, 193-203, doi:10.1038/nrmicro2522 (2011).

8 Garfoot, A. L. & Rappleye, C. A. Histoplasma capsulatum surmounts obstacles to intracellular pathogenesis. *FEBS J* **283**, 619-633, doi:10.1111/febs.13389 (2016).

9 Seider, K. *et al.* The facultative intracellular pathogen Candida glabrata subverts macrophage cytokine production and phagolysosome maturation. *J Immunol* **187**, 3072-3086, doi:10.4049/jimmunol.1003730 (2011).

10 Bain, J. M. *et al.* Non-lytic expulsion/exocytosis of Candida albicans from macrophages. *Fungal genetics and biology : FG & B* **49**, 677-678, doi:10.1016/j.fgb.2012.01.008 (2012).

11 Ma, H., Croudace, J. E., Lammas, D. A. & May, R. C. Expulsion of live pathogenic yeast by macrophages. *Curr Biol* **16**, 2156-2160, doi:10.1016/j.cub.2006.09.032 (2006).

12 Alvarez, M. & Casadevall, A. Phagosome extrusion and host-cell survival after Cryptococcus neoformans phagocytosis by macrophages. *Curr Biol* **16**, 2161-2165, doi:10.1016/j.cub.2006.09.061 (2006).

13 O'Meara, T. R. *et al.* Global analysis of fungal morphology exposes mechanisms of host cell escape. *Nature communications* **6**, 6741, doi:10.1038/ncomms7741 (2015).

14 Ibrahim-Granet, O. *et al.* Phagocytosis and intracellular fate of Aspergillus fumigatus conidia in alveolar macrophages. *Infect Immun* **71**, 891-903 (2003).

15 Lee, S. C. *et al.* Calcineurin orchestrates dimorphic transitions, antifungal drug responses and host-pathogen interactions of the pathogenic mucoralean fungus Mucor circinelloides. *Mol Microbiol* **97**, 844-865, doi:10.1111/mmi.13071 (2015).

16 Aimanianda, V. & Latge, J. P. Fungal hydrophobins form a sheath preventing immune recognition of airborne conidia. *Virulence* **1**, 185-187, doi:10.4161/viru.1.3.11317 (2010).

17 Aimanianda, V. *et al.* Surface hydrophobin prevents immune recognition of airborne fungal spores. *Nature* **460**, 1117-1121, doi:10.1038/nature08264 (2009).

18 Ibrahim, A. S. & Voelz, K. The mucormycete-host interface. *Curr Opin Microbiol* **40**, 40-45, doi:10.1016/j.mib.2017.10.010 (2017).

19 Skiada, A., Rigopoulos, D., Larios, G., Petrikkos, G. & Katsambas, A. Global epidemiology of cutaneous zygomycosis. *Clin Dermatol* **30**, 628-632, doi:10.1016/j.clindermatol.2012.01.010 (2012).

20 Blyth, C. C. *et al.* Consensus guidelines for the treatment of invasive mould infections in haematological malignancy and haemopoietic stem cell transplantation, 2014. *Internal medicine journal* **44**, 1333-1349, doi:10.1111/imj.12598 (2014).

21 Roden, M. M. *et al.* Epidemiology and outcome of zygomycosis: a review of 929 reported cases. *Clin Infect Dis* **41**, 634-653, doi:10.1086/432579 (2005).

22 de Hoog, S., Ibrahim, A. S. & Voigt, K. Zygomycetes: an emerging problem in the clinical laboratory. *Mycoses* **57 Suppl 3**, 1, doi:10.1111/myc.12285 10.1111/myc.12250 (2014).

23 Douglas, A. P., Chen, S. C. & Slavin, M. A. Emerging infections caused by non-Aspergillus filamentous fungi. *Clin Microbiol Infect* **22**, 670-680, doi:10.1016/j.cmi.2016.01.011 (2016).

24 Gomes, M. Z., Lewis, R. E. & Kontoyiannis, D. P. Mucormycosis caused by unusual mucormycetes, non-Rhizopus, -Mucor, and -Lichtheimia species. *Clin Microbiol Rev* **24**, 411-445, doi:10.1128/cmr.00056-10 (2011).

25 Kontoyiannis, D. P. & Lewis, R. E. Invasive zygomycosis: update on pathogenesis, clinical manifestations, and management. *Infect Dis Clin North Am* **20**, 581-607, vi, doi:10.1016/j.idc.2006.06.003 (2006).

26 Petraitis, V. *et al.* Increased virulence of Cunninghamella bertholletiae in experimental pulmonary mucormycosis: correlation with circulating molecular biomarkers, sporangiospore germination and hyphal metabolism. *Med Mycol* **51**, 72-82, doi:10.3109/13693786.2012.690107 (2013).

27 Li, C. H. *et al.* Sporangiospore size dimorphism is linked to virulence of Mucor circinelloides. *PLoS Pathog* **7**, e1002086, doi:10.1371/journal.ppat.1002086 (2011).

28 Antachopoulos, C., Demchok, J. P., Roilides, E. & Walsh, T. J. Fungal biomass is a key factor affecting polymorphonuclear leucocyte-induced hyphal damage of filamentous fungi. *Mycoses* **53**, 321-328, doi:10.1111/j.1439-0507.2009.01725.x (2010).

29 Schmidt, S. *et al.* Rhizopus oryzae hyphae are damaged by human natural killer (NK) cells, but suppress NK cell mediated immunity. *Immunobiology* **218**, 939-944, doi:10.1016/j.imbio.2012.10.013 (2013).

30 Schmidt, S., Schneider, A., Demir, A., Lass-Florl, C. & Lehrnbecher, T. Natural killer cell-mediated damage of clinical isolates of mucormycetes. *Mycoses* **59**, 34-38, doi:10.1111/myc.12431 (2016).

31 Chander, J. *et al.* Mucormycosis: Battle with the Deadly Enemy over a Five-Year Period in India. *J Fungi (Basel)* **4**, doi:10.3390/jof4020046 (2018).

32 Dolatabadi, S., Kolecka, A., Versteeg, M., de Hoog, S. G. & Boekhout, T. Differentiation of clinically relevant Mucorales Rhizopus microsporus and R. arrhizus by matrix-assisted laser desorption ionization time-of-flight mass spectrometry (MALDI-TOF MS). *Journal of medical microbiology* **64**, 694-701, doi:10.1099/jmm.0.000091 (2015).

33 Chamilos, G. *et al.* Generation of IL-23 producing dendritic cells (DCs) by airborne fungi regulates fungal pathogenicity via the induction of T(H)-17 responses. *PLoS One* **5**, e12955, doi:10.1371/journal.pone.0012955 (2010).

34 Chayakulkeeree, M., Ghannoum, M. A. & Perfect, J. R. Zygomycosis: the re-emerging fungal infection. *European journal of clinical microbiology & infectious diseases : official publication of the European Society of Clinical Microbiology* **25**, 215-229, doi:10.1007/s10096-006-0107-1 (2006).

35 Ibrahim, A. S. *et al.* Bacterial endosymbiosis is widely present among zygomycetes but does not contribute to the pathogenesis of mucormycosis. *J Infect Dis* **198**, 1083-1090, doi:10.1086/591461 (2008).

36 Gebremariam, T. *et al.* CotH3 mediates fungal invasion of host cells during mucormycosis. *J Clin Invest* **124**, 237-250, doi:10.1172/jci71349 (2014).

37 Baldin, C. & Ibrahim, A. S. Molecular mechanisms of mucormycosis-The bitter and the sweet. *PLoS Pathog* **13**, e1006408, doi:10.1371/journal.ppat.1006408 (2017).

38 Gleissner, B., Schilling, A., Anagnostopolous, I., Siehl, I. & Thiel, E. Improved outcome of zygomycosis in patients with hematological diseases? *Leukemia & lymphoma* **45**, 1351-1360, doi:10.1080/10428190310001653691 (2004).

39 Celis-Aguilar, E. *et al.* An Emergent Entity: Indolent Mucormycosis of the Paranasal Sinuses. A Multicenter Study. *Int Arch Otorhinolaryngol* **23**, 92-100, doi:10.1055/s-0038-1667005 (2019).

40 Andrianaki, A. M. *et al.* Iron restriction inside macrophages regulates pulmonary host defense against Rhizopus species. *Nature communications* **9**, 3333, doi:10.1038/s41467-018-05820-2 (2018).

41 Inglesfield, S. *et al.* Robust Phagocyte Recruitment Controls the Opportunistic Fungal Pathogen Mucor circinelloides in Innate Granulomas In Vivo. *MBio* **9**, doi:10.1128/mBio.02010-17 (2018).

42 Ibrahim, A. S. & Kontoyiannis, D. P. Update on mucormycosis pathogenesis. *Curr Opin Infect Dis* **26**, 508-515, doi:10.1097/qco.0000000000000008 (2013).

43 Ibrahim, A. S., Spellberg, B. & Edwards, J., Jr. Iron acquisition: a novel perspective on mucormycosis pathogenesis and treatment. *Curr Opin Infect Dis* **21**, 620-625, doi:10.1097/QCO.0b013e3283165fd1 (2008).

44 Ibrahim, A. S., Spellberg, B., Walsh, T. J. & Kontoyiannis, D. P. Pathogenesis of mucormycosis. *Clin Infect Dis* **54 Suppl 1**, S16-22, doi:10.1093/cid/cir865 (2012).

45 Mendoza, L. *et al.* Human Fungal Pathogens of Mucorales and Entomophthorales. *Cold Spring Harb Perspect Med* **5**, doi:10.1101/cshperspect.a019562 (2015).

46 Kontoyiannis, D. P. *et al.* Future directions in mucormycosis research. *Clin Infect Dis* **54 Suppl 1**, S79-85, doi:10.1093/cid/cir886 (2012).

47 Kaur, R., Bala, K., Ahuja, R. B., Srivastav, P. & Bansal, U. Primary cutaneous mucormycosis in a patient with burn wounds due to Lichtheimia ramosa. *Mycopathologia* **178**, 291-295, doi:10.1007/s11046-014-9805-x (2014).

48 Kennedy, K. J. *et al.* Mucormycosis in Australia: contemporary epidemiology and outcomes. *Clin Microbiol Infect*, doi:10.1016/j.cmi.2016.01.005 (2016).

49 Mohindra, S., Gupta, B., Gupta, K. & Bal, A. Tracheal mucormycosis pneumonia: a rare clinical presentation. *Respiratory care* **59**, e178-181, doi:10.4187/respcare.03174 (2014).

50 Novosad, S. A. *et al.* Notes From the Field: Probable Mucormycosis Among Adult Solid Organ Transplant Recipients at an Acute Care Hospital - Pennsylvania, 2014-

2015. *American journal of transplantation : official journal of the American Society of Transplantation and the American Society of Transplant Surgeons* **16**, 2758-2759, doi:10.1111/ajt.13990 (2016).

51 Gartenberg, G., Bottone, E. J., Keusch, G. T. & Weitzman, I. Hospital-acquired mucormycosis (Rhizopus rhizopodiformis) of skin and subcutaneous tissue: epidemiology, mycology and treatment. *N Engl J Med* **299**, 1115-1118, doi:10.1056/NEJM197811162992007 (1978).

52 Maravi-Poma, E. *et al.* Outbreak of gastric mucormycosis associated with the use of wooden tongue depressors in critically ill patients. *Intensive care medicine* **30**, 724-728, doi:10.1007/s00134-003-2132-1 (2004).

53 Mitchell, S. J., Gray, J., Morgan, M. E., Hocking, M. D. & Durbin, G. M. Nosocomial infection with Rhizopus microsporus in preterm infants: association with wooden tongue depressors. *Lancet* **348**, 441-443 (1996).

54 Paydas, S. *et al.* Mucormycosis of the tongue in a patient with acute lymphoblastic leukemia: a possible relation with use of a tongue depressor. *Am J Med* **114**, 618-620 (2003).

55 Cheng, V. C. *et al.* Outbreak of intestinal infection due to Rhizopus microsporus. *J Clin Microbiol* **47**, 2834-2843, doi:10.1128/JCM.00908-09 (2009).

56 Kobayashi, D. Y. & Crouch, J. A. Bacterial/Fungal interactions: from pathogens to mutualistic endosymbionts. *Annu Rev Phytopathol* **47**, 63-82, doi:10.1146/annurev-phyto-080508-081729 (2009).

57 Spraker, J. E., Sanchez, L. M., Lowe, T. M., Dorrestein, P. C. & Keller, N. P. Ralstonia solanacearum lipopeptide induces chlamydospore development in fungi and facilitates bacterial entry into fungal tissues. *ISME J* **10**, 2317-2330, doi:10.1038/ismej.2016.32 (2016).

58 Mondo, S. J. *et al.* Bacterial endosymbionts influence host sexuality and reveal reproductive genes of early divergent fungi. *Nature communications* **8**, 1843, doi:10.1038/s41467-017-02052-8 (2017).

59 Partida-Martinez, L. P. & Hertweck, C. Pathogenic fungus harbours endosymbiotic bacteria for toxin production. *Nature* **437**, 884-888, doi:10.1038/nature03997 (2005).

60 Partida-Martinez, L. P. *et al.* Rhizonin, the first mycotoxin isolated from the zygomycota, is not a fungal metabolite but is produced by bacterial endosymbionts. *Appl Environ Microbiol* **73**, 793-797, doi:10.1128/aem.01784-06 (2007).

61 Medwid, R. D. & Grant, D. W. Germination of Rhizopus oligosporus Sporangiospores. *Appl Environ Microbiol* **48**, 1067-1071 (1984).

62 Chamilos, G. *et al.* Drosophila melanogaster as a model host to dissect the immunopathogenesis of zygomycosis. *Proceedings of the National Academy of Sciences of the United States of America* **105**, 9367-9372, doi:10.1073/pnas.0709578105 (2008).

63 Griffin, D. H. *Fungal Physiology, 2nd ed.* . (Wiley-Liss, , 1994).

64 Voelz, K., Gratacap, R. L. & Wheeler, R. T. A zebrafish larval model reveals early tissue-specific innate immune responses to Mucor circinelloides. *Dis Model Mech* **8**, 1375-1388, doi:10.1242/dmm.019992 (2015).

65 Waldorf, A. R. & Diamond, R. D. Neutrophil chemotactic responses induced by fresh and swollen Rhizopus oryzae spores and Aspergillus fumigatus conidia. *Infect Immun* **48**, 458-463 (1985).

66 Turgeman, T. *et al.* The Role of Aquaporins in pH-Dependent Germination of Rhizopus delemar Spores. *PLoS One* **11**, e0150543, doi:10.1371/journal.pone.0150543 (2016).

67 Thau, N. *et al.* rodletless mutants of Aspergillus fumigatus. *Infect Immun* **62**, 4380-4388 (1994).

68 Jennessen, J., Schnurer, J., Olsson, J., Samson, R. A. & Dijksterhuis, J. Morphological characteristics of sporangiospores of the tempe fungus Rhizopus oligosporus differentiate it from other taxa of the R. microsporus group. *Mycol Res* **112**, 547-563, doi:10.1016/j.mycres.2007.11.006 (2008).

69 Waldorf, A. R., Levitz, S. M. & Diamond, R. D. In vivo bronchoalveolar macrophage defense against Rhizopus oryzae and Aspergillus fumigatus. *J Infect Dis* **150**, 752-760 (1984).

70 Waldorf, A. R., Peter, L. & Polak, A. Mucormycotic infection in mice following prolonged incubation of spores in vivo and the role of spore agglutinating antibodies on spore germination. *Sabouraudia* **22**, 101-108 (1984).

71 Waldorf, A. R., Ruderman, N. & Diamond, R. D. Specific susceptibility to mucormycosis in murine diabetes and bronchoalveolar macrophage defense against Rhizopus. *J Clin Invest* **74**, 150-160, doi:10.1172/JCI111395 (1984).

72 Sephton-Clark, P. *et al.* Host-pathogen transcriptomics of macrophages, Mucorales and their endosymbionts: a polymicrobial pas de trois. *BioRXiv*, doi: https://doi.org/10.1101/580746 (2019).

73 Wurster, S. *et al.* Mucorales spores induce a proinflammatory cytokine response in human mononuclear phagocytes and harbor no rodlet hydrophobins. *Virulence* **8**, 1708-1718, doi:10.1080/21505594.2017.1342920 (2017).

74 Chamilos, G., Lewis, R. E., Lamaris, G. A., Albert, N. D. & Kontoyiannis, D. P. Genomewide screening for genes associated with gliotoxin resistance and sensitivity in Saccharomyces cerevisiae. *Antimicrob Agents Chemother* **52**, 1325-1329, doi:10.1128/AAC.01393-07 (2008).

75 Tominaga, Y. & Tsujisaka, Y. Investigation of the Structure of Rhizopus Cell Wall with Lytic Enzymes. *Agricultural and Biological Chemistry* **45**, 1569-1575, doi:10.1080/00021369.1981.10864749 (1981).

76 Kinchen, J. M. & Ravichandran, K. S. Phagosome maturation: going through the acid test. *Nature reviews. Molecular cell biology* **9**, 781-795, doi:10.1038/nrm2515 (2008).

77 Gotthardt, D. *et al.* High-resolution dissection of phagosome maturation reveals distinct membrane trafficking phases. *Mol Biol Cell* **13**, 3508-3520, doi:10.1091/mbc.e02-04-0206 (2002).

78 Partida-Martinez, L. P., Bandemer, S., Ruchel, R., Dannaoui, E. & Hertweck, C. Lack of evidence of endosymbiotic toxin-producing bacteria in clinical Rhizopus isolates. *Mycoses* **51**, 266-269, doi:10.1111/j.1439-0507.2007.01477.x (2008).

79 Prota, A. E. *et al.* A new tubulin-binding site and pharmacophore for microtubule-destabilizing anticancer drugs. *Proc Natl Acad Sci U S A* **111**, 13817-13821, doi:10.1073/pnas.1408124111 (2014).

80 Takahashi, M. *et al.* Rhizoxin binding to tubulin at the maytansine-binding site. *Biochim Biophys Acta* **926**, 215-223 (1987).

81 Partida-Martinez, L. P. *et al.* Burkholderia rhizoxinica sp. nov. and Burkholderia endofungorum sp. nov., bacterial endosymbionts of the plant-pathogenic fungus

Rhizopus microsporus. *Int J Syst Evol Microbiol* **57**, 2583-2590, doi:10.1099/ijs.0.64660-0 (2007).

82 Partida-Martinez, L. P. & Hertweck, C. A gene cluster encoding rhizoxin biosynthesis in "Burkholderia rhizoxina", the bacterial endosymbiont of the fungus Rhizopus microsporus. *Chembiochem : a European journal of chemical biology* **8**, 41-45, doi:10.1002/cbic.200600393 (2007).

83 Zhang, L., Morrison, M. & Rickard, C. M. Draft Genome Sequence of Ralstonia pickettii AU12-08, Isolated from an Intravascular Catheter in Australia. *Genome Announc* **2**, doi:10.1128/genomeA.00027-14 (2014).

84 Chen, Y. Y. *et al.* An Outbreak of Ralstonia pickettii Bloodstream Infection Associated with an Intrinsically Contaminated Normal Saline Solution. *Infection control and hospital epidemiology* **38**, 444-448, doi:10.1017/ice.2016.327 (2017).

85 Tejera, D., Limongi, G., Bertullo, M. & Cancela, M. Ralstonia pickettii bacteremia in hemodialysis patients: a report of two cases. *Rev Bras Ter Intensiva* **28**, 195-198, doi:10.5935/0103-507X.20160033 (2016).

86 Ryan, M. P. & Adley, C. C. The antibiotic susceptibility of water-based bacteria Ralstonia pickettii and Ralstonia insidiosa. *Journal of medical microbiology* **62**, 1025-1031, doi:10.1099/jmm.0.054759-0 (2013).

87 Steenbergen, J. N., Shuman, H. A. & Casadevall, A. Cryptococcus neoformans interactions with amoebae suggest an explanation for its virulence and intracellular pathogenic strategy in macrophages. *Proc Natl Acad Sci U S A* **98**, 15245-15250, doi:10.1073/pnas.261418798 (2001).

88 Watkins, R. A. *et al.* Cryptococcus neoformans Escape From Dictyostelium Amoeba by Both WASH-Mediated Constitutive Exocytosis and Vomocytosis. *Frontiers in cellular and infection microbiology* **8**, 108, doi:10.3389/fcimb.2018.00108 (2018).

89 Ashworth, J. M. & Watts, D. J. Metabolism of the cellular slime mould Dictyostelium discoideum grown in axenic culture. *Biochem J* **119**, 175-182 (1970).

90 Scherlach, K., Partida-Martinez, L. P., Dahse, H. M. & Hertweck, C. Antimitotic rhizoxin derivatives from a cultured bacterial endosymbiont of the rice pathogenic fungus Rhizopus microsporus. *Journal of the American Chemical Society* **128**, 11529-11536, doi:10.1021/ja062953o (2006).

91 Blin, K. *et al.* antiSMASH 4.0-improvements in chemistry prediction and gene cluster boundary identification. *Nucleic Acids Res* **45**, W36-W41, doi:10.1093/nar/gkx319 (2017).

92 Renshaw, S. A. *et al.* A transgenic zebrafish model of neutrophilic inflammation. *Blood* **108**, 3976-3978, doi:10.1182/blood-2006-05-024075 (2006).

93 Ellett, F., Pase, L., Hayman, J. W., Andrianopoulos, A. & Lieschke, G. J. mpeg1 promoter transgenes direct macrophage-lineage expression in zebrafish. *Blood* **117**, e49-56, doi:10.1182/blood-2010-10-314120 (2011).

94 Shaffer, J. P., U'Ren, J. M., Gallery, R. E., Baltrus, D. A. & Arnold, A. E. An Endohyphal Bacterium (Chitinophaga, Bacteroidetes) Alters Carbon Source Use by Fusarium keratoplasticum (F. solani Species Complex, Nectriaceae). *Front Microbiol* **8**, 350, doi:10.3389/fmicb.2017.00350 (2017).

95 Husnik, F. & McCutcheon, J. P. Functional horizontal gene transfer from bacteria to eukaryotes. *Nat Rev Microbiol* **16**, 67-79, doi:10.1038/nrmicro.2017.137 (2018).

96 Hoffman, M. T., Gunatilaka, M. K., Wijeratne, K., Gunatilaka, L. & Arnold, A. E. Endohyphal bacterium enhances production of indole-3-acetic acid by a foliar fungal endophyte. *PLoS One* **8**, e73132, doi:10.1371/journal.pone.0073132 (2013).

97 Frey-Klett, P. *et al.* Bacterial-fungal interactions: hyphens between agricultural, clinical, environmental, and food microbiologists. *Microbiol Mol Biol Rev* **75**, 583-609, doi:10.1128/mmbr.00020-11 (2011).

98 Araldi-Brondolo, S. J. *et al.* Bacterial Endosymbionts: Master Modulators of Fungal Phenotypes. *Microbiology spectrum* **5**, doi:10.1128/microbiolspec.FUNK-0056-2016 (2017).

99 Moebius, N., Uzum, Z., Dijksterhuis, J., Lackner, G. & Hertweck, C. Active invasion of bacteria into living fungal cells. *Elife* **3**, e03007, doi:10.7554/eLife.03007 (2014).

100 Uehling, J. *et al.* Comparative genomics of Mortierella elongata and its bacterial endosymbiont Mycoavidus cysteinexigens. *Environmental microbiology* **19**, 2964-2983, doi:10.1111/1462-2920.13669 (2017).

101 Takashima, Y. *et al.* Prevalence and Intra-Family Phylogenetic Divergence of Burkholderiaceae-Related Endobacteria Associated with Species of Mortierella. *Microbes Environ*, doi:10.1264/jsme2.ME18081 (2018).

102 Gee, J. E. *et al.* Characterization of Burkholderia rhizoxinica and B. endofungorum isolated from clinical specimens. *PLoS One* **6**, e15731, doi:10.1371/journal.pone.0015731 (2011).

103 Nazir, R., Tazetdinova, D. I. & van Elsas, J. D. Burkholderia terrae BS001 migrates proficiently with diverse fungal hosts through soil and provides protection from antifungal agents. *Frontiers in microbiology* **5**, 598, doi:10.3389/fmicb.2014.00598 (2014).

104 Benoit, I. *et al.* Bacillus subtilis attachment to Aspergillus niger hyphae results in mutually altered metabolism. *Environ Microbiol* **17**, 2099-2113, doi:10.1111/1462-2920.12564 (2015).

105 Zheng, H., Dietrich, C. & Brune, A. Genome Analysis of Endomicrobium proavitum Suggests Loss and Gain of Relevant Functions during the Evolution of Intracellular Symbionts. *Appl Environ Microbiol* **83**, doi:10.1128/aem.00656-17 (2017).

106 Salvioli, A. *et al.* Symbiosis with an endobacterium increases the fitness of a mycorrhizal fungus, raising its bioenergetic potential. *The ISME journal* **10**, 130-144, doi:10.1038/ismej.2015.91 (2016).

107 Lackner, G., Partida-Martinez, L. P. & Hertweck, C. Endofungal bacteria as producers of mycotoxins. *Trends Microbiol* **17**, 570-576, doi:10.1016/j.tim.2009.09.003 (2009).

108 Sharmin, D. *et al.* Comparative Genomic Insights into Endofungal Lifestyles of Two Bacterial Endosymbionts, Mycoavidus cysteinexigens and Burkholderia rhizoxinica. *Microbes Environ* **33**, 66-76, doi:10.1264/jsme2.ME17138 (2018).

109 Kontoyiannis, D. P., Wessel, V. C., Bodey, G. P. & Rolston, K. V. Zygomycosis in the 1990s in a tertiary-care cancer center. *Clin Infect Dis* **30**, 851-856, doi:10.1086/313803 (2000).

110 Liu, X. H. *et al.* Autophagy-related protein MoAtg14 is involved in differentiation, development and pathogenicity in the rice blast fungus Magnaporthe oryzae. *Scientific reports* **7**, 40018, doi:10.1038/srep40018 (2017).

111 Brunet, K., Alanio, A., Lortholary, O. & Rammaert, B. Reactivation of dormant/latent fungal infection. *Journal of Infection*, doi:10.1016/j.jinf.2018.06.016 (2018).

112 Ralph, P., Prichard, J. & Cohn, M. Reticulum cell sarcoma: an effector cell in antibody-dependent cell-mediated immunity. *Journal of immunology (Baltimore, Md. : 1950)* **114**, 898-905 (1975).

113 Smith, L. M., Dixon, E. F. & May, R. C. The fungal pathogen Cryptococcus neoformans manipulates macrophage phagosome maturation. *Cell Microbiol* **17**, 702-713, doi:10.1111/cmi.12394 (2015).

114 Sephton-Clark, P. C. S., Munoz, J. F., Ballou, E. R., Cuomo, C. A. & Voelz, K. Pathways of Pathogenicity: Transcriptional Stages of Germination in the Fatal Fungal Pathogen Rhizopus delemar. *mSphere* **3**, doi:10.1128/mSphere.00403-18 (2018).

115 Brothers, K. M., Newman, Z. R. & Wheeler, R. T. Live imaging of disseminated candidiasis in zebrafish reveals role of phagocyte oxidase in limiting filamentous growth. *Eukaryot Cell* **10**, 932-944, doi:10.1128/EC.05005-11 (2011).

116 Kimmel, C. B., Ballard, W. W., Kimmel, S. R., Ullmann, B. & Schilling, T. F. Stages of embryonic development of the zebrafish. *Dev Dyn* **203**, 253-310, doi:10.1002/aja.1002030302 (1995).

FIGURE 1: Resting spores are readily phagocytosed, yet swollen spores inhibit macrophage function. A) Phagocytosis of resting and swollen (2 and 4 h) spores by J774A.1 macrophages. B) Total Chitin (CFW) and Mannan (ConA) exposure in resting and swollen spores analysed by flow cytometry (>10,000 cells), including Median Fluorescence Intensity (left) and Percent High (right) for each population. Data representative of three independent repeats is shown. **C**) Effect of swollen spore supernatant on phagocytic uptake of resting spores of *R. microsporus* by macrophages. **D**) Phagocytosis of resting and swollen spores of other mucoralean fungal species (M.c. = *Mucor circinelloides f. lusitanicus*). **E**) Effect of supernatants collected from swollen spores from other mucormycetes on phagocytosis of resting spores of *R. microsporus* by macrophages. **F**) Effect of swollen spore supernatants from the indicated species on phagocytosis of *Candida albicans* and *Saccharomyces cerevisiae* by macrophages. For all assays, the number of phagocytes containing at least one spore were counted after 1 hour (n=3000, One way ANOVA with Tukey's correction for multiple comparisons). In each graph, three biological replicates were examined and error bars represent s.e.m. (***** = $p<0.05$, ** $p<0.001$,*** = $p<0.0001$).

FIGURE 2. *R. microsporus* culture supernatant can inhibit macrophage function. (A) Percent spore killing by macrophages following phagocytic uptake. One way ANOVA with Tukey's correction for multiple comparisons (n=3 biological replicates). **(B)** Quantification of phagosome maturation following phagocytic uptake of live or killed spores. **(C)** Effect of supernatant treatment on cell morphology (rounding). **(D, E)** Effect of supernatant treatment on (**D**), actin polymerization measured by staining with rhodamine-conjugated phalloidin and **(E)** tubulin polymerization measured by staining with anti-beta tubulin antibody. Representative micrographs are shown. (**B,C,D,E**) Analyzed using Student's two-tailed T-test with Welsh's correction for unequal variance (n=100 (**B,D,E**), 150 (**C**) per replicate, with three biological replicates). For all graphs, data shown are mean with s.e.m. (*** $p < 0.0001$).

Figure 3: *R. microsporus* is colonised by a bacterial endosymbiont, *R. pickettii* A) Genomic DNA was isolated from parent and cured clinical R. microsporus (FP469-12) and control (CBS-631.82) fungal and isolated bacteria strains as indicated and screened by PCR for the amplification of a 1.5 kb band indicative of presence of bacterial 16S rDNA. Representative gel image is shown. **B)** Spores of parent and cured strains of *R. microsporus* FP469-12 were fermented in VK medium, the mycelial pellet submerged in NaCl and then stained with SYTO9 to reveal bacterial endosymbionts. Representative micrographs are

shown. **C)** Genomic DNA was isolated from both parent and cured strains of the indicated mucoralean fungi and screened by PCR for the amplification of a 1.5 kb band indicative of bacterial 16S rDNA. A representative gel image is shown. *Rd: R. delemar; Rc: R. chinensis; Lc: L. corymbifera; Cb: C. bartholletiae; MC: M. circinelloides f. lusitanicus CBS-277490; MN: M. circinelloides f. lusitanicus NRRL-3631* All data are representative of three independent biological repeats.

Figure 4: The bacterial endosymbiont influences fungal secretome and interaction with mammalian cells in vitro. A) Phagocytosis of parent or cured resting or swollen (2 and 4 h) spores of *R. microsporus* FP469-12 by J774A.1 macrophages (n=3 biological replicates, One way ANOVA with Tukey's correction for multiple comparisons). **B)** Effect of bacterial endosymbiont supernatants isolated from indicated fungal hosts on phagocytosis of *R. microsporus* resting spores. **C)** Effect of filtered supernatants from co-cultures of bacterial symbionts and cured fungal spores grown in DMEM on phagocytosis of *R. microsporus* resting spores. For assays **A-C**, the number of phagocytes containing at least one spore were counted at the indicated time points. (n=3000). **Di-Dii)** Effect of supernatants from parent or cured fungal (*R. microsporus* FP469-12) and bacterial (*R. pickettii*) strains on phagosome maturation, and actin and tubulin polymerisation. For assays Di-Diii, n=50, One Way ANOVA with Tukey's correction for multiple comparisons. In each graph, three biological repeats were examined and error bars represent s.e.m. (***** = $p<0.05$, **=$p<0.001$, *** = $p<0.0001$).

Figure 5: The endosymbiont influences fungal cell wall organisation. Ai) Impact of bacterial endosymbionts on fungal (*R. microsporus* F469-12) parent or cured spores survival following co-co-culture with J774A.1 macrophage for the indicated time points**. Aii, iii)** Impact of bacterial endosymbionts on fungal (*R. microsporus* F469-12) parent or cured resting spores susceptibility to stress factors include cell wall, nitrosative, oxidative and antifungal stresses at the indicated concentrations. Three biological repeats were examined and error bars represent s.e.m. Statistical significance was assessed via One way ANOVA with Tukey's correction for multiple comparisons (**=$p<0.001$, ***=$p=0.0001$, ****=$p<0.00001$). **B)** Effect of endosymbiont status on *R. microsporus* F469-12 fungal structure. The TEM microraphs represent cross-sectional structures of both the parent and cured swollen spores, plus close up of the fungal cell wall in both cases. **C**) Effect of endosymbiont cure on cell wall stain uptake during germination for total chitin (Calcofluor White), exposed chitin (Wheat-Germ Agglutinin), mannan (Concanavalin A) and total protein (FITC) (n=300 for each).

Figure 6. *R. microsporus* secretes a hydrophobic compound that antagonizes effect functions of macrophages and is dependent on *R. pickettii*. (**A**) High performance liquid chromatography (HPLC) profiles of chloroform-extracted swollen spore supernatant and DMEM medium control showing the three most active peaks. **B)** Effect of individual fractionated HPLC peaks on phagocytic uptake of resting spores of *R. microsporus* F469-12 by J774A.1 macrophages. **C)** HPLC profiles of rhizoxin D control; and cured *R. microsporus F469-12*, bacterial symbiont (*R. pickettii*), parent *R. microsporus* F469-12 cultivated in DMEM. **D)** Effect of bacterial *(R. picketti)*, cured fungal (Rm FP 469-12) supernatant and Rhizoxin D control on phagocytosis of resting spores of Rm (FP 469-12) by J77.4 macrophages. For **B** and **D**, the number of phagocytes containing at least one spore were counted at the indicated time points (n=3000, One way ANOVA with Tukey's correction for multiple comparisons). In each graph, three biological repeats were examined and error bars repesent s.e.m. where (**=$p<0.001$ and ***=$p<0.0001$). **E)** HPLC profiles of chloroform-extracted bacterial (*R. pickettii*) supernantant cultivated in HL5 medium (positive) or VK

medium (negative) and media only controls. The culture extracts were monitored at 210 nm, and chromatograms are representative from at least three biological repeats. **F**) Volcano plot comparing RNAseq data across inducing (DMEM+fungus and HL-5) vs. non-inducing (VK and DMEM) conditions. Differentially expressed genes identified in red are those with an FDR of <0.001 and Log Fold Change ±2.

Figure 7: The secreted factor is distinct from Rhizo-toxins. (**A.B**) Effect of bacterial (*R. pickettii*) and cured fungal (*R. microsporus* FP469-12) supernatants and rhizoxin D (3 *p*M) on **A)** actin polymerisation, and **B)** β-tubulin polymerisation. Representative micrographs are show. (One way ANOVA with Tukey's correction for multiple comparisons; n=50 cells per replicate, with three biological replicates. Data shown are mean with s.e.m. (*** = p<0.0001).

Figure 8. Bacterial-fungal symbiosis enables fungal survival *in vivo*. A) Effect of endosymbiont status on survival of AB wildtype zebrafish injected via the hindbrain with wild type or cured resting or swollen spores of *R. microsporus* FP469-12. Three biological replicates of populations of 10 fish each were examined (n=30). Statistical differences were determined using Mantel-Cox with Bonferroni's correction for multiple comparisons (5% family-wise significance threshold = 0.025). **B)** Effect of endosymbiont status on fungal survival (CFUs) following hindbrain injections of AB wild type zebrafish with wild type or cured resting (i) or swollen (ii) *R. microsporus* FP469-12 spores. Three biological replicates of populations of 5 fish per condition were examined (n=15). **C,D)** Effect of bacterial symbiont on macrophage **(C)** or neutrophil **(D)** recruitment to the site of infection following injection of parent or cured resting (i) or swollen (ii) spores. Three biological replicates of populations of 4 fish per condition were examined (n=12). **B-D)** Statistical significance was assessed by Two-way ANOVA with Tukey's correction for multiple comparisons or pairwise t-tests where sample number was unequal due to fish death (**C**,D 48 hr, 72hr swollen spores) (*=p<0.05; **=p<0.001; ***=p<0.0001 unless otherwise indicated). **E)** Effect of endosymbiont status on fungal survival (CFUs) following intra-tracheal infection of mice at 4 and 48 hours with resting spores (n=5). Statistical significance was determined using the Mann-Whitney test. **F)** Relative risk of CFU status (positive vs below the limit of detection) for mice 48 hours post-infection with untreated vs. pre-treated (60 μg/ml Ciprofloxacin, 3hr) resting spores. Statistical significance was assessed using a 2-sided Chi-squared test, and Attributable Risk was assessed using Newcombe/Wilson with continuity correction) (*=p=0.384).

Supplemental figures

Table S1 Average spore diameter (μm). Spore diameter was measured for the indicated strains at the indicated times. n=300

Figure S2 Impact of spore size and UV killing on Phagocytosis. A) Phagocytosis of spores is not affected by size. Phagocytosis of swollen (4h, 6.5 μm) parent *R. microsporus* FP 469-12 spores and latex beads (11.9 μm) by J774A.1 macrophages. The number of phagocytes containing at least one spore were counted at the indicated time points (n=3000, One way ANOVA with Tukey's correction for multiple comparisons) Three biological repeats were examined and error bars represent s.e.m. (***=p<0.0001). **B)** Phagocytosis of spores is restored when spores are UV

killed. Phagocytosis of UV inactivated parent resting and swollen *R. microsporus* FP 469-12 spores by J774A.1 macrophages. The number of phagocytes containing at least one spore were counted at the indicated time points (n=3000, One way ANOVA with Tukey's correction for multiple comparisons) Three biological repeats were examined and error bars represent s.e.m. (ns = p>0.05).

Figure S3 Cell wall staining of resting and swollen spores for total (CFW) and exposed (WGA) chitin, or total protein (FITC). Resting *R. microsporus* FP 469-12 spores were pre-germinated at the indicated time points with the indicated fluorophores, visualized by fluorescence microscopy and stain uptake for individual spores quantified. (n=300, One-Way ANOVA with Tukey's correction for multiple comparisons). Three biological repeats were examined and error bars represent s.e.m (ns = p>0.05, ***=p<0.0001).

Figure S4 Cell wall staining of resting and swollen spores for β-glucan (dectin-1). Resting *R. microsporus* FP 469-12 spores were pre-germinated at the indicated time points, fixed in 4% methanol-free formaldehyde, and incubated with Dectin-1 IgG antibody followed by goat anti-mouse IgG-488 secondary antibody. Binding was assessed for at least 10,000 cells via flow cytometry compared to a pooled secondary-only control. Data are representative of three independent experiments.

Figure S5 A) Characterisation of macrophages untreated or treated with swollen spore supernatant. A) Quantification of phagosome maturation (lysotracker red) after uptake of killed spores in the presence or absence of supernatant from swollen *R. microsporus* FP 469-12 spores. **B)** Quantification of cell viability by LDH release following treatment of J774A.1 macrophages with swollen spore supernatant. Cell lysis buffer (positive) and DMEM only (negative) treated cells serve as controls. **C)** Quantification of macrophage viability by Trypan blue staining following treatment with swollen spore supernatant. For all graphs, 100 cells with phagocytosed spores from three biological repeats were examined; error bars represent s.d**.** where (***=p<0.0001).

Supplemental Figure S6 Effect of digestion, boiling and oxidation on supernatant activity. **A)** Effect of the indicated treatments on the activity of swollen *R. microsporus* FP 469-12 spore supernatant against phagocytosis of resting *R. microsporus* FP 469-12 spores by J774A.1 macrophages. **B)** Level of activity of total chloroform extracted R. microsporus *FP 469-12* supernatant from swollen spores against phagocytosis of resting *R. microsporus* FP 469-12 spores by J774A.1 macrophages. The number of phagocytes containing at least one spore were counted at the indicated time points (n=3000, One way ANOVA with Tukey's correction for multiple comparisons) Three biological repeats per treatment condition were examined and data represent s.e.m. where (**=p=0.009, ***=p<0.0001)

Supplemental Figure S7 High resolution mass spectrometry profiles of active HPLC peaks and Rhizoxin D control. A) MS profile of Peak 5 the most active against phagocytosis. B) MS profile of peak 8 the next moderately active against phagocytosis **C)** MS profile for peak 3 the least active against phagocytosis. Three biological repeats were examined. **D)** Rhizoxin D is a reference standard.

Supplemental Figure S8 A) Spore CFU from swollen spores in infected fish. A) Average survival of parent and cured resting and swollen fungal spores following infection of zebrafish (n=15 per group). Three biological repeats of 5 fish per group were examined

(n=15)**.** All data presented in Figure 8 are shown on a single graph for comparisons across conditions. B) Kaplan-Meyer Survival curves for MPEG (Macrophage) and MPO (Neutrophil) fish. Transgenic zebrafish were infected with wild type or cured strains of *R. microsporus* by injecting into the hindbrain. Injected fish were then cultivated in E3 medium and monitored every 24 h.p.i for total of 96 h.p.i with mortality rates assessed every 24 h.p.i. (n=12). Statistical differences were determined using Mantel-Cox with Bonferroni's correction for multiple comparisons (5% family-wise significance threshold = 0.025). C,D) Effect of bacterial symbiont on macrophage (C) and neutrophil (D) recruitment to the site of infection following injection of parent or cured resting or swollen spores. Three biological replicates of populations of 4 fish per condition were examined (n=12). All data presented in Figure 8 are shown on a single graph for comparison across conditions. **A, C,D)** Statistical significance was assessed by Two-way ANOVA with Tukey's correction for multiple comparisons. **E)** Kaplan-Meyer Survival curves for impact of 60 μg/ml ciprofloxacin on survival in infected wildtype AB fish. Zebrafish were infected with wild type *R. microsporus* spores by injecting into the hindbrain (n=30). Injected fish were then cultivated in E3 medium with or without 60 μg/ml Ciprofloxacin and monitored every 24 h.p.i for total of 96 h.p.i with mortality rates assessed every 24 h.p.i. (n=12). Statistical differences were determined using Mantel-Cox with Bonferroni's correction for multiple comparisons (5% family-wise significance threshold = 0.025). **F)** Effect of endosymbiont status on fungal survival (CFUs) following intra-tracheal infection of mice at 4 and 48 hours with swollen spores (n=5). Statistical significance was determined using the Mann-Whitney test. **G)** Relative risk of CFU status (positive vs below the limit of detection) for mice 48 hours post-infection with untreated vs. pre-treated (60 μg/ml Ciprofloxacin, 3hr) swollen spores. Statistical significance was assessed using a 2-sided Chi-squared test, and Attributable Risk was assessed using Newcombe/Wilson with continuity correction) (ns=p=0>0.05)).

Supplemental Figure S9 Zebrafish larvae infection model. Representative micrographs of zebrafish larvae infected with CFW-stained swollen parent spores as analyzed in Figure 8 for A) AB WT fish at time of infection, and over the indicated times in B) MPEG (Macrophage, red) and C) MPO (Neutrophil, green) fish.

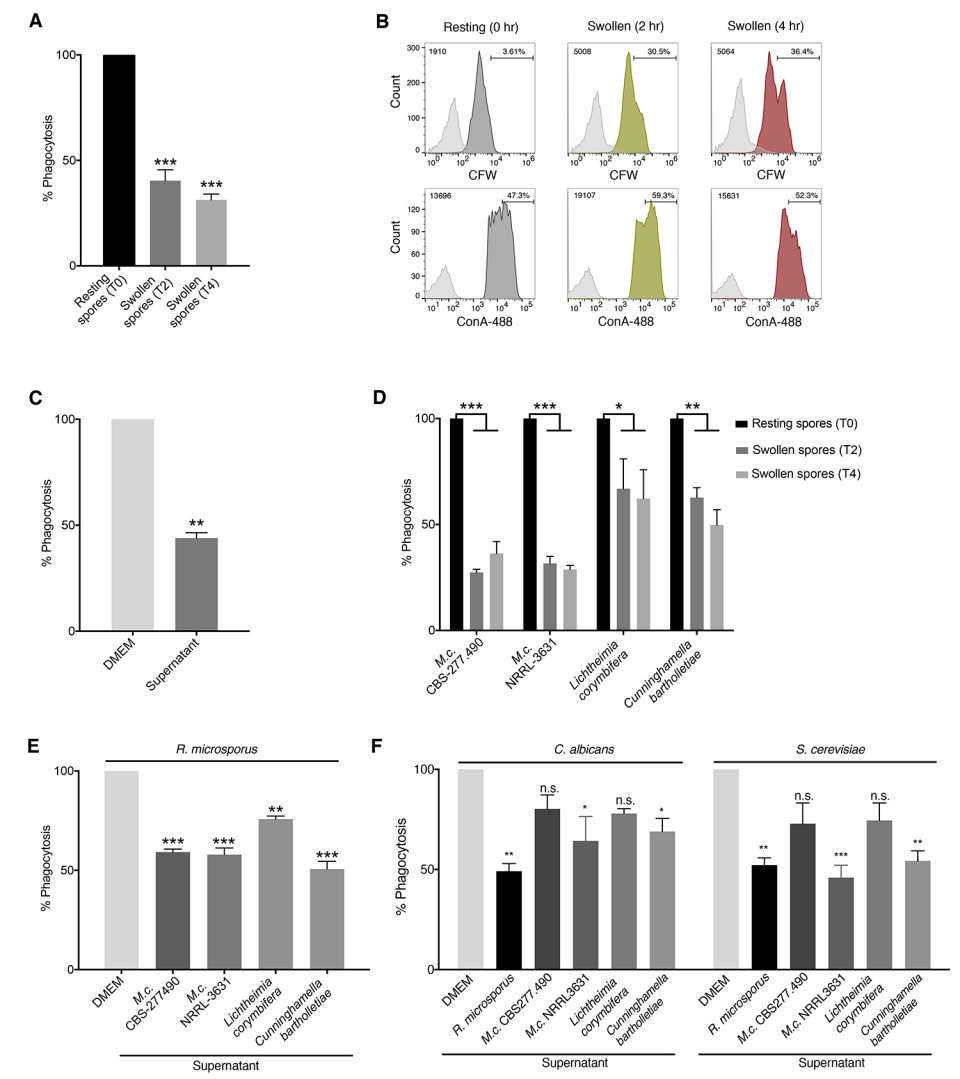
A
% Phagocytosis
100
50
0
***
***
Resting spores (T0)
Swollen spores (T2)
Swollen spores (T4)
B
Resting (0 hr)
Swollen (2 hr)
Swollen (4 hr)
Count
1910
3.61%
5008
30.5%
5064
36.4%
CFW
13696
47.3%
19107
59.3%
15631
52.3%
ConA-488
C
% Phagocytosis
100
50
0
**
DMEM
Supernatant
D
% Phagocytosis
***
***
*
**
Resting spores (T0)
Swollen spores (T2)
Swollen spores (T4)
M.c. CBS-277.490
M.c. NRRL-3631
Lichtheimia corymbifera
Cunninghamella bartholletiae
E
R. microsporus
% Phagocytosis
***
***
**
***
DMEM
M.c. CBS-277490
M.c. NRRL-3631
Lichtheimia corymbifera
Cunninghamella bartholletiae
Supernatant
F
C. albicans
S. cerevisiae
% Phagocytosis
**
n.s.
*
n.s.
*
**
n.s.
***
n.s.
**
DMEM
R. microsporus
M.c. CBS277.490
M.c. NRRL3631
Lichtheimia corymbifera
Cunninghamella bartholletiae
Supernatant

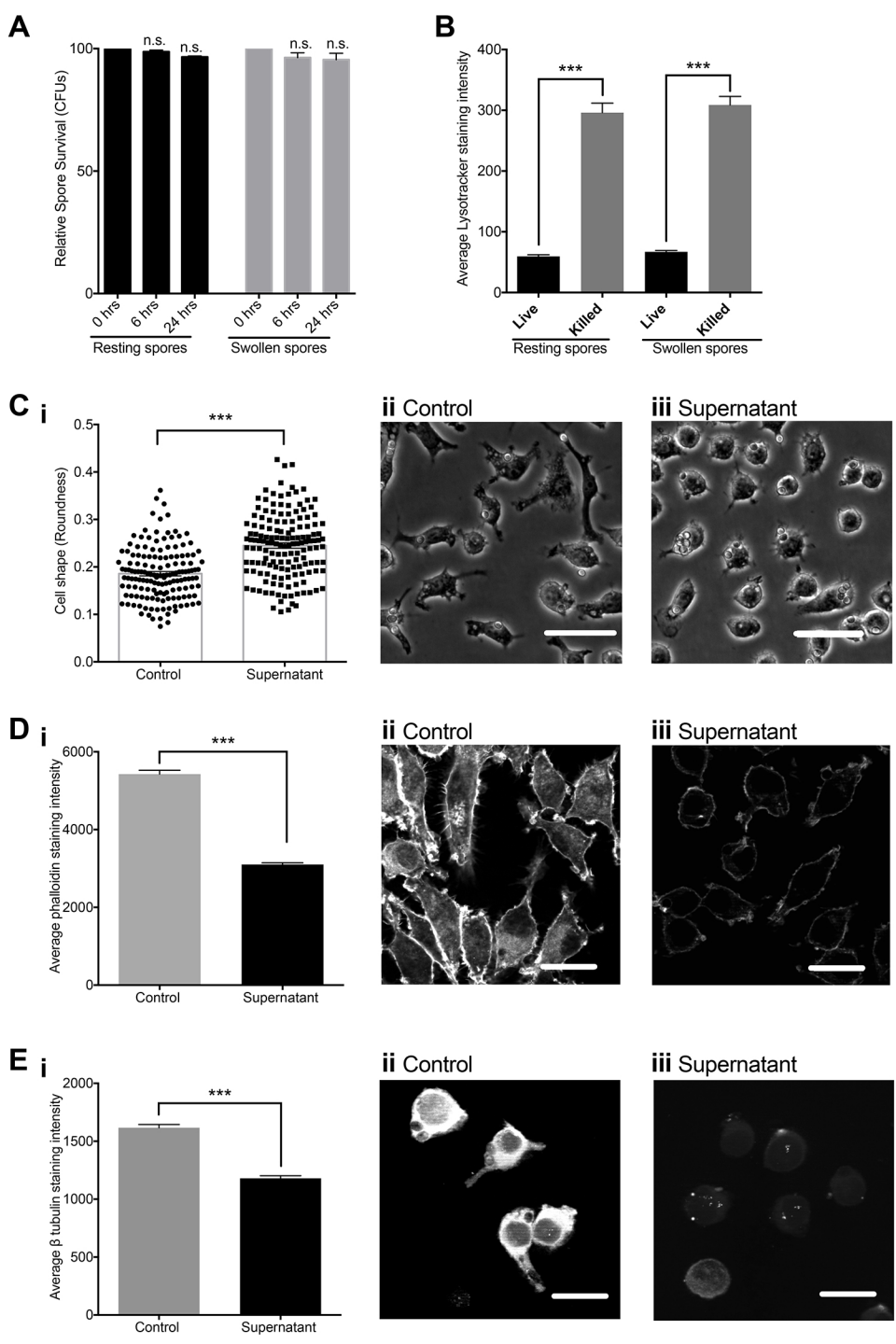
A
Relative Spore Survival (CFUs)
100
50
0
n.s.
n.s.
n.s.
n.s.
0 hrs
6 hrs
24 hrs
0 hrs
6 hrs
24 hrs
Resting spores
Swollen spores
B
Average Lysotracker staining intensity
400
300
200
100
0
***
***
Live
Killed
Live
Killed
Resting spores
Swollen spores
C
i
Cell shape (Roundness)
0.5
0.4
0.3
0.2
0.1
0.0
***
Control
Supernatant
ii Control
iii Supernatant
D
i
Average phalloidin staining intensity
6000
4000
2000
0
***
Control
Supernatant
ii Control
iii Supernatant
E
i
Average β tubulin staining intensity
2000
1500
1000
500
0
***
Control
Supernatant
ii Control
iii Supernatant

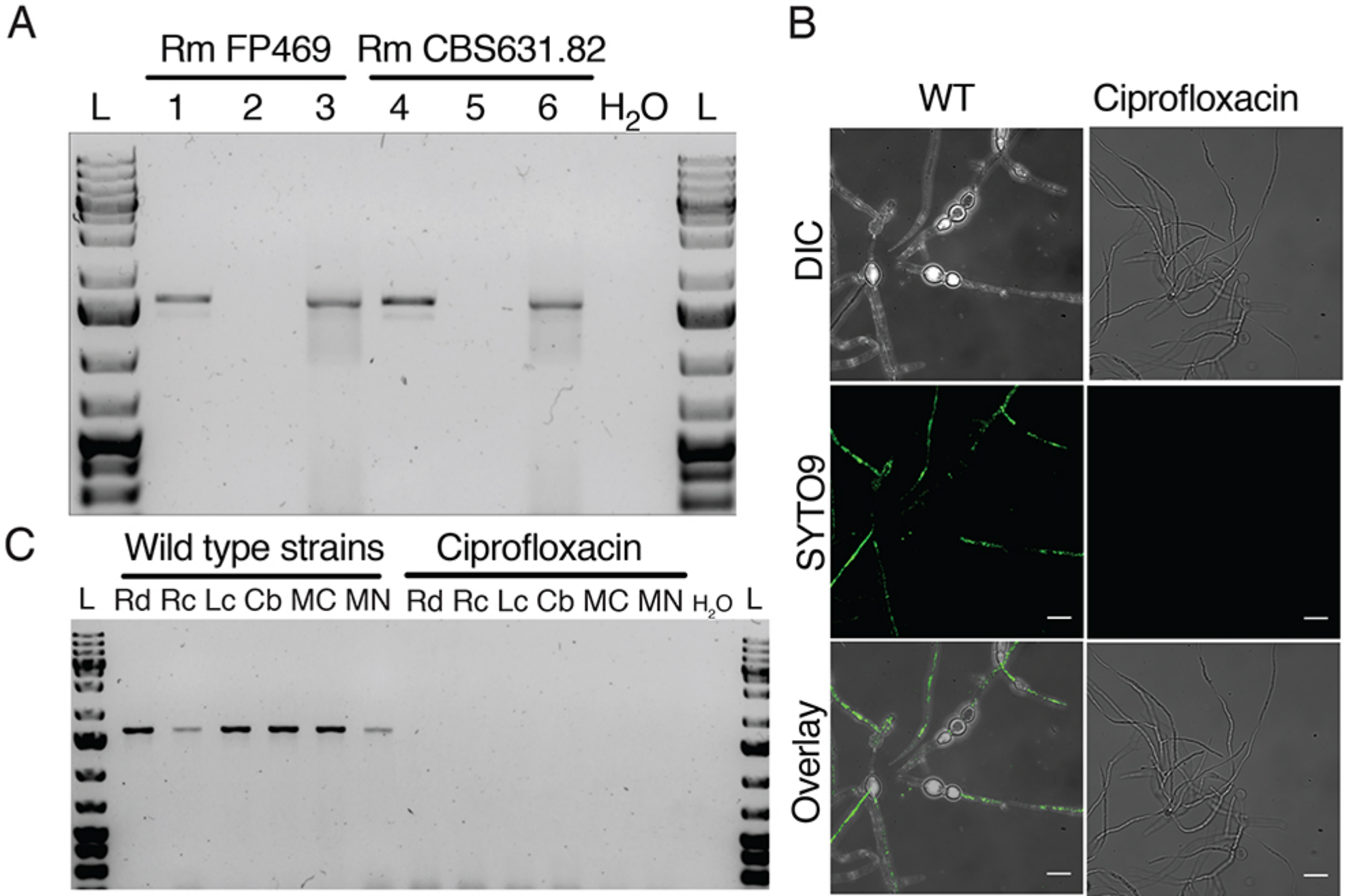
A
Rm FP469
Rm CBS631.82
L
1
2
3
4
5
6
H2O
L
B
WT
Ciprofloxacin
DIC
SYTO9
Overlay
C
Wild type strains
Ciprofloxacin
L
Rd
Rc
Lc
Cb
MC
MN
Rd
Rc
Lc
Cb
MC
MN
H2O
L

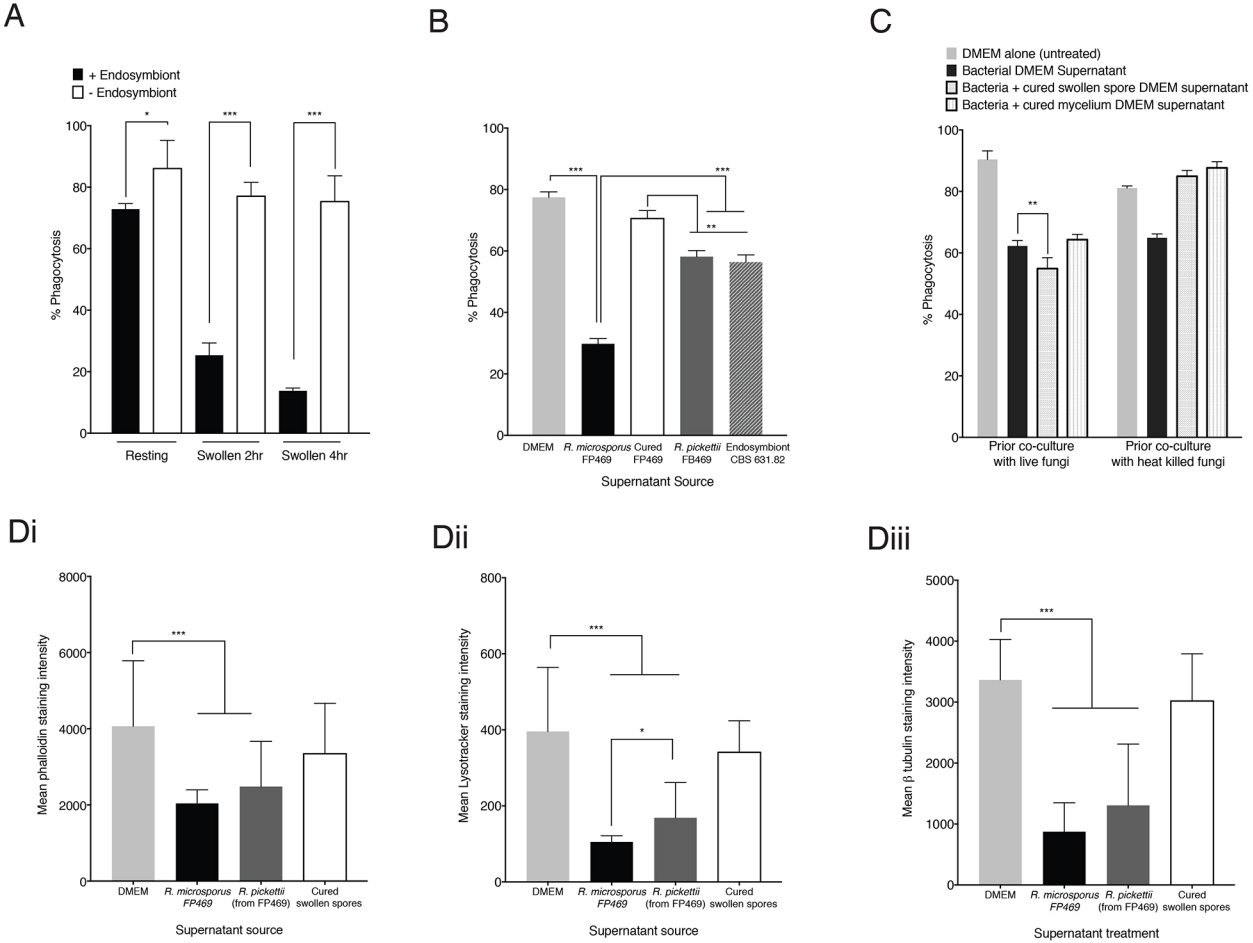
A
+ Endosymbiont
- Endosymbiont
% Phagocytosis
Resting
Swollen 2hr
Swollen 4hr
B
% Phagocytosis
DMEM
R. microsporus FP469
Cured FP469
R. pickettii FB469
Endosymbiont CBS 631.82
Supernatant Source
C
DMEM alone (untreated)
Bacterial DMEM Supernatant
Bacteria + cured swollen spore DMEM supernatant
Bacteria + cured mycelium DMEM supernatant
% Phagocytosis
Prior co-culture with live fungi
Prior co-culture with heat killed fungi
Di
Mean phalloidin staining intensity
DMEM
R. microsporus FP469
R. pickettii (from FP469)
Cured swollen spores
Supernatant source
Dii
Mean Lysotracker staining intensity
DMEM
R. microsporus FP469
R. pickettii (from FP469)
Cured swollen spores
Supernatant source
Diii
Mean β tubulin staining intensity
DMEM
R. microsporus FP469
R. pickettii (from FP469)
Cured swollen spores
Supernatant treatment

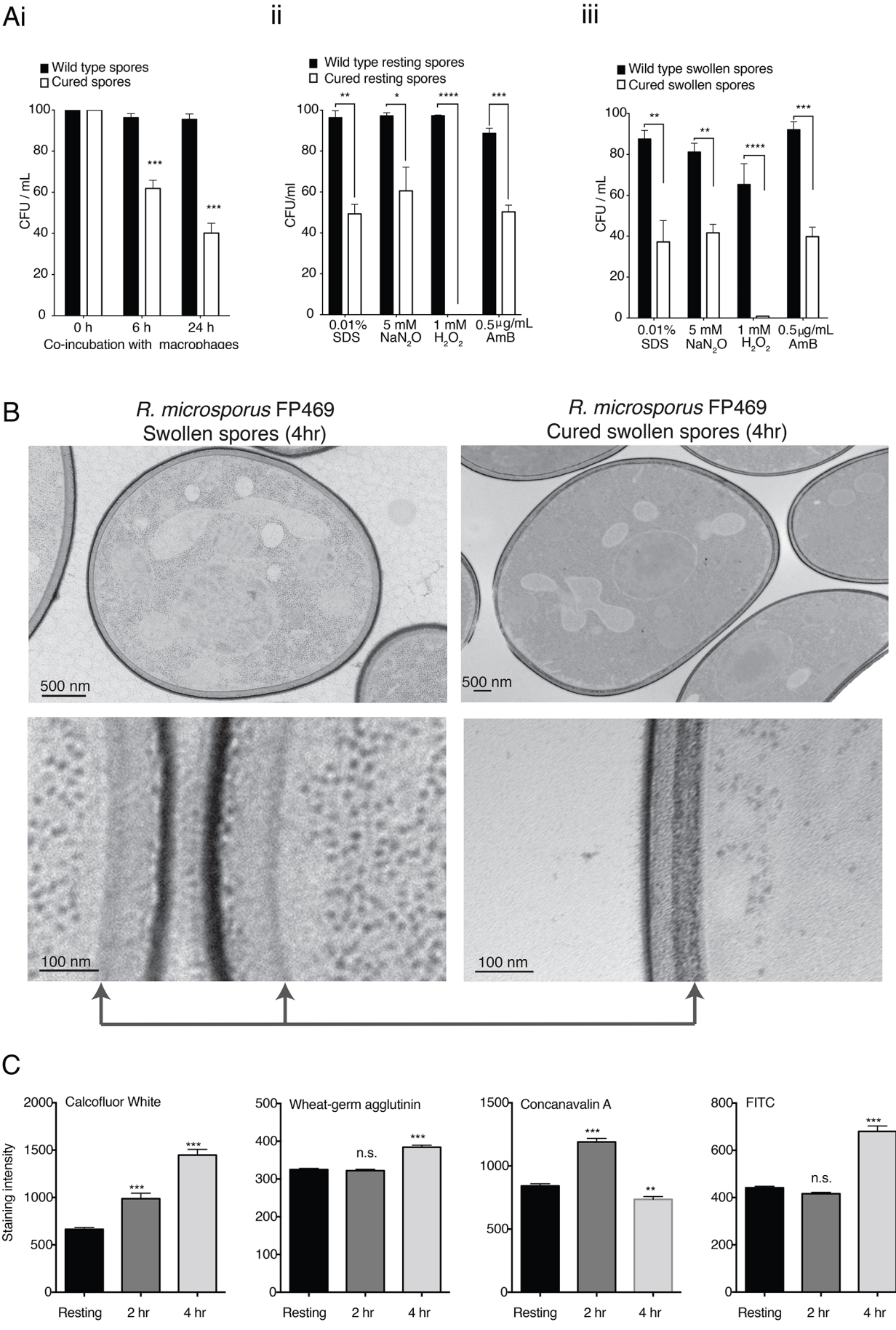
Ai
ii
iii
Wild type spores
Cured spores
CFU / mL
0 h
6 h
24 h
Co-incubation with macrophages
Wild type resting spores
Cured resting spores
CFU/ml
0.01% SDS
5 mM NaN2O
1 mM H2O2
0.5µg/mL AmB
Wild type swollen spores
Cured swollen spores
B
R. microsporus FP469
Swollen spores (4hr)
R. microsporus FP469
Cured swollen spores (4hr)
500 nm
100 nm
C
Staining intensity
Calcofluor White
Wheat-germ agglutinin
Concanavalin A
FITC
n.s.
Resting
2 hr
4 hr

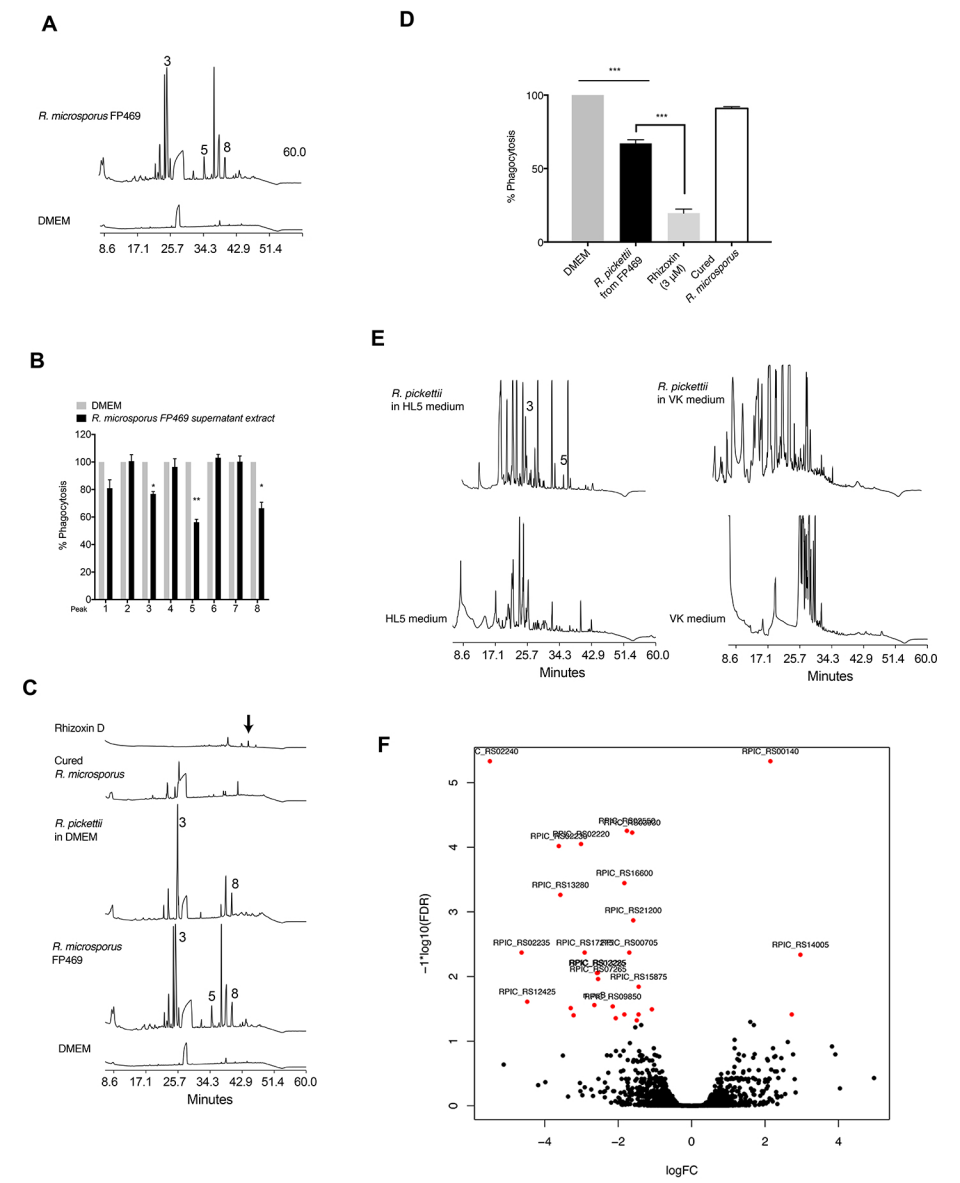
A
R. microsporus FP469
3
5
8
60.0
DMEM
8.6 17.1 25.7 34.3 42.9 51.4
D
***
***
100
50
0
% Phagocytosis
DMEM
R. pickettii from FP469
Rhizoxin (3 μM)
Cured R. microsporus
B
DMEM
R. microsporus FP469 supernatant extract
120
100
80
60
40
20
0
% Phagocytosis
*
**
*
Peak 1 2 3 4 5 6 7 8
E
R. pickettii in HL5 medium
3
5
R. pickettii in VK medium
HL5 medium
VK medium
8.6 17.1 25.7 34.3 42.9 51.4 60.0
Minutes
8.6 17.1 25.7 34.3 42.9 51.4 60.0
Minutes
C
Rhizoxin D
Cured R. microsporus
R. pickettii in DMEM
3
8
R. microsporus FP469
3
5
8
DMEM
8.6 17.1 25.7 34.3 42.9 51.4 60.0
Minutes
F
RPIC_RS02240
RPIC_RS00140
RPIC_RS02220
RPIC_RS16600
RPIC_RS13280
RPIC_RS21200
RPIC_RS02235
RPIC_RS00705
RPIC_RS14005
RPIC_RS07265
RPIC_RS15875
RPIC_RS12425
RPIC_RS09850
−1*log10(FDR)
5
4
3
2
1
0
−4
−2
0
2
4
logFC

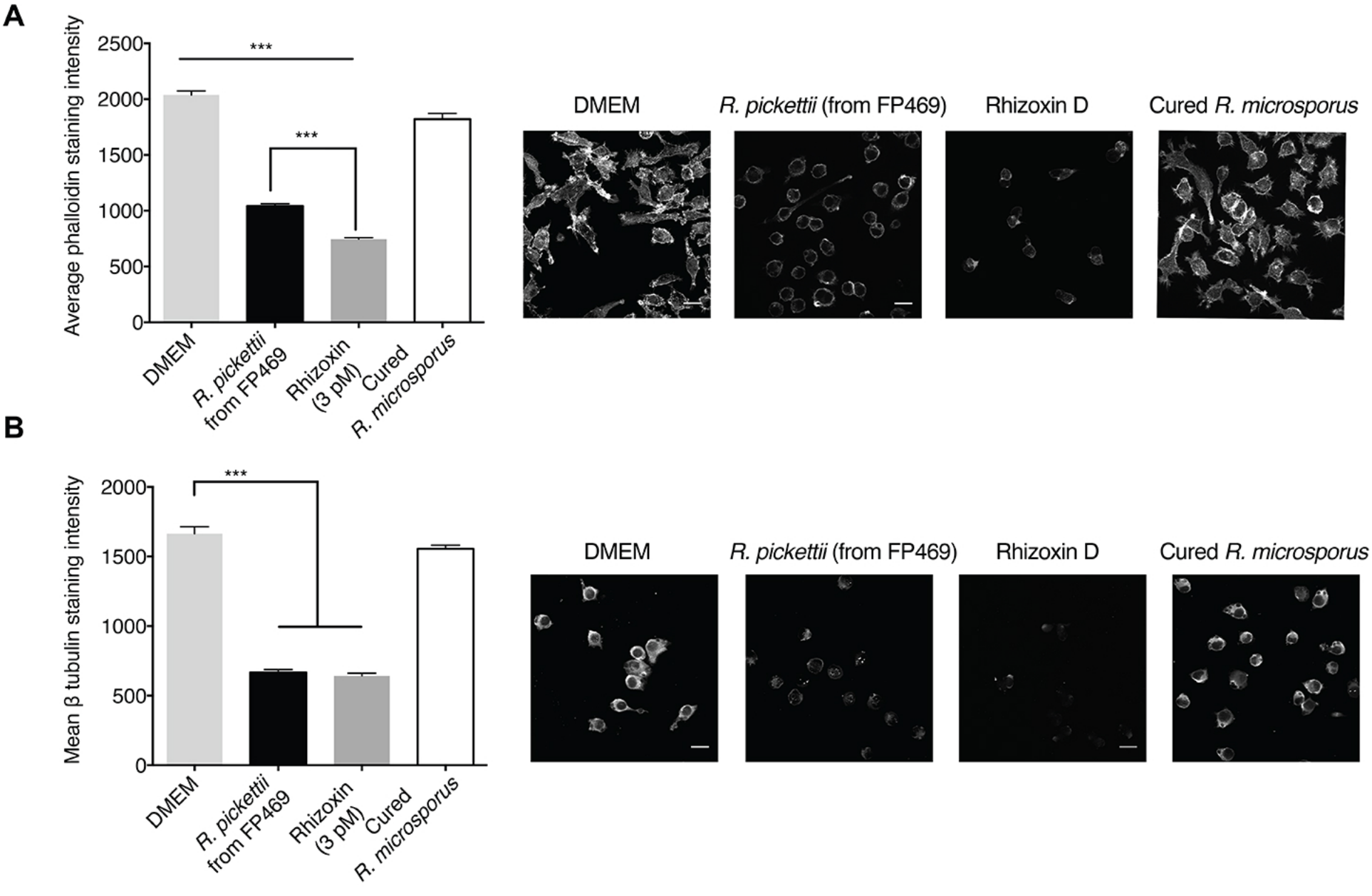
A
Average phalloidin staining intensity
2500
2000
1500
1000
500
0
***
***
DMEM
R. pickettii from FP469
Rhizoxin (3 pM)
Cured R. microsporus
DMEM
R. pickettii (from FP469)
Rhizoxin D
Cured R. microsporus
B
Mean β tubulin staining intensity
2000
1500
1000
500
0
***
DMEM
R. pickettii from FP469
Rhizoxin (3 pM)
Cured R. microsporus
DMEM
R. pickettii (from FP469)
Rhizoxin D
Cured R. microsporus

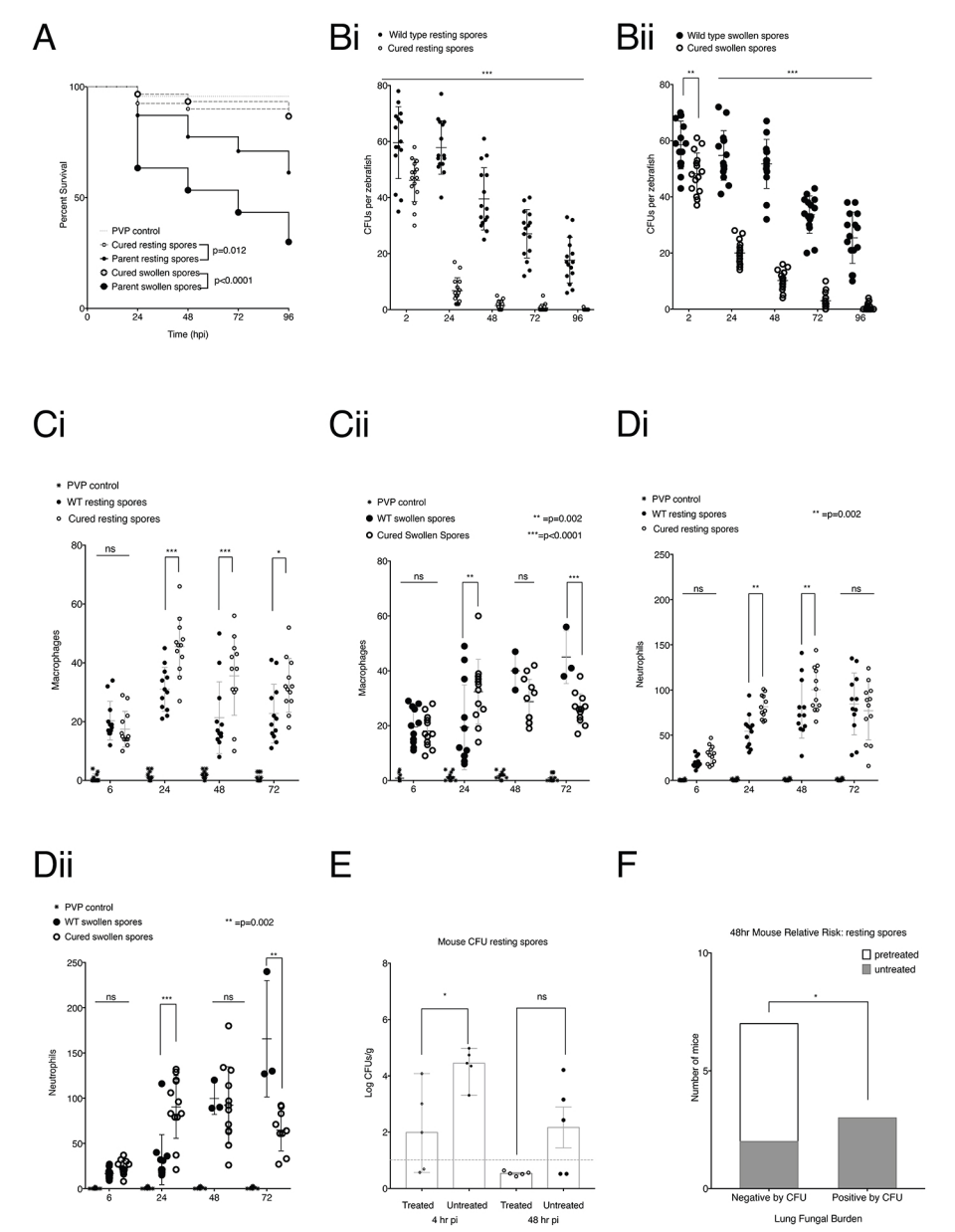
A
Percent Survival
Time (hpi)
PVP control
Cured resting spores
Parent resting spores
Cured swollen spores
Parent swollen spores
p=0.012
p<0.0001
Bi
Wild type resting spores
Cured resting spores
CFUs per zebrafish
Bii
Wild type swollen spores
Cured swollen spores
CFUs per zebrafish
Ci
PVP control
WT resting spores
Cured resting spores
Macrophages
Cii
PVP control
WT swollen spores
Cured Swollen Spores
** =p=0.002
***=p<0.0001
Macrophages
Di
PVP control
WT resting spores
Cured resting spores
** =p=0.002
Neutrophils
Dii
PVP control
WT swollen spores
Cured swollen spores
** =p=0.002
Neutrophils
E
Mouse CFU resting spores
Log CFUs/g
Treated
Untreated
4 hr pi
48 hr pi
F
48hr Mouse Relative Risk: resting spores
pretreated
untreated
Number of mice
Negative by CFU
Positive by CFU
Lung Fungal Burden